Spring 1-1-2017

Harness Surface Morphologies for Optical Applications

Yinding Chi
University of Colorado at Boulder, john_chiyd@hotmail.com

HARNESS SURFACE MORPHOLOGIES FOR OPTICAL APPLICATIONS

by

YINDING CHI

B.S., Huazhong University of Science and Technology, 2014

A thesis submitted to the

Faculty of the Graduate School of the

University of Colorado in partial fulfillment

of the requirement for the degree of

Master of Science

Department of Mechanical Engineering

2017

This thesis entitled:

Harness Surface Morphologies for Optical Applications

written by Yinding Chi

has been approved for the Department of Mechanical Engineering

_____

Prof.Jianliang Xiao

_____

Prof. Yifu Ding

Date_____

The final copy of this thesis has been examined by the signatories, and we find that both the content and the form meet acceptable presentation standards

of scholarly work in the above mentioned discipline.

Yinding Chi (M.S. Mechanical Engineering)

Harness Surface Morphologies for Optical Applications

Thesis is directed by Professor Jianliang Xiao

Abstract

Industrial and technology in advanced promote the development of optical system towards accessible to be high-performance, robust and easy to be tunable. Nowadays, with the development of precision manufacturing, the surface morphologies can be modified in micro scale even nano-scale which are in conformity with the requirement of the optical systems or devices. In this dissertation, several surficial morphology-based compatible and tunable optical systems have been put forward with simple dynamic actuation with the potential applications in smart window, optical diffuser and optical grating.

First of all, an optimal etching time has been explored in a wrinkling-cracking based tunable smart window application. With the increased UVO etching time, the thickness of top oxidized layer enhanced a lot. As the uniaxial strain applied, the surface morphology is variable. By the comparison of different UVO etched situations, the optimal UVO treating time for smart window sample with largest tunable transmittance has be raised. Moreover, the tunable transmittance range versus UVO treating time has been developed as a consequence.

Additional discover is that the micro-scaled sinusoidal surface has a scattering effect for transmitted light source when we went through the first project. Therefore, a high-performance optical diffuser with novel screwthread-like wrinkling morphology is fabricated simply and cheaply based on two arrays of micro-scaled wrinkling patterns perpendicular to each other. Such optical diffuser can scatter the light uniformly in a rectangular region, with a high haze performance. Furthermore, two-sided surface modified optical diffuser is demonstrated to enhance the optical performance with a much larger scattering region. The scattering region can also be tuned from rectangular shape to one-dimensional line via simple mechanical actuation as well.

Last but not the least, a series of hierarchical surface architectures are fabricated by combining the micro-scaled wrinkling pattern with sub-micro-scaled wavy structure. Such morphology cannot only diffuse the transmitting light but also perform the tunable diffraction phenomenon for potential optical grating application. In additional, a high-performance optical diffuser (scattering angle ~60°) is exhibited via two optical grating samples stacking together.

This dissertation is dedicated to my grandfather Jichao Chi, my parents Xueli Chi and Pei Cai.

Acknowledgement

My dissertation would not accomplished without help, guidance, and support from many people. I'd like to take this opportunity to express my gratitude to thank all contributed to my success during my M.S. study.

First, I would like to express my deepest gratitude to my dearest advisor, Dr. Jianliang Xiao for his all-time support, encouragement, and guidance. I never forget the moment that he teach me how to make a presentation, how to write a paper, and how to solve and analyze a scientific problem which will continuously contribute for my academic career. Besides, I want to thank Prof. Xiao for his strong recommendation in my PhD's application.

Secondly, I also want to thank Prof. Yifu Ding and Prof. Francisco Lopez for agreeing to serve as my thesis defense committee. I gratefully appreciate their advice and comments for my dissertation. I also want to thank to Prof. YC Lee, and Prof. Victor Bright for their strong recommendations in my PhD's application.

In addition, I would like to thank to my collaborators: First, special thanks to Dr. Zhengwei Li from my group. He is not my collaborator but also a guider as well. Thanks for his all-time advice and comments on my research.

Besides, thanks to Yao Zhai and Hang Yin from Prof. Xiaobo Yin's group to help me measure optical properties and set up observation stage.

Also, I would like to thank to my lab-mates Yu Wang, Zhanan Zou, Qingyang Sun, Yan Li, Chuanqian Shi, Andres Villada, and Sichong Li to their help for

my research studies. It's my great honor to work with so many intelligent minds.

Finally, I would express my love to my family. My parents, thanks them for their long-time support and encouragement during my study. I'm grateful for their scarification and love. I owe them a lot.

Contents

Tables

Table

Figures

Figure

Chapter 1 Introduction

1.1. Surface wrinkling morphologies

Wrinkling or folded phenomenon is very common in daily routine, for example, the wavy structural geomorphology, wrinkling tiles for Chinese

traditional architecture, and wrinkles on human skin. With the development of micro fabrication and accurate manufacturing, the micro scaled wrinkling surface morphology has been exhibited for a wide range of potential applications: stretchable electronics [1-3], measurement of mechanical properties[4,5], novel hydrophobic structure, and optical devices[6,7].

Different fabrication approaches has been introduced to induce wrinkling or wavy surface morphologies through thermal mismatch [8-10], mechanical strain mismatch [11-14], focused ion beam [15], ultraviolet ozone and oxygen plasma surface treatment [16-19] and others [20-24]. Figure 1-1 a) shows the preparation of wrinkling surface by mechanical strain mismatch [11]. The Si thin film seats on mother wafer with photoresist toughed onto the Si film, after the top exposed Si was etched away, the Si ribbons formed. And then, a pre-stretched elastomeric polydimethylsiloxane (PDMS) bonded conformably with the Si ribbons. After peeling off the PDMS bonded with Si ribbons, the deformable wrinkling pattern formed on both PDMS substrate and Si film when the strain released. Figure1-1 c) shows uniform wrinkling pattern of Si-PDMS sample via scanning electron microscope. After that, novel two-dimensional wrinkling morphology has been developed by J. Song in 2008 [25]. Figure 1-2 a) shows such fabrication process: first, the Si membrane is bonded onto the top of two-dimensional pre-strain applied PDMS by a series of photolithography processes. After releasing the pre-strain, the PDMS slab recovered to its initial state which induce two-dimensional wavy pattern on

the surface of Si membrane. Figure1.2 b) shows micrographs of its spatially distributed morphology.

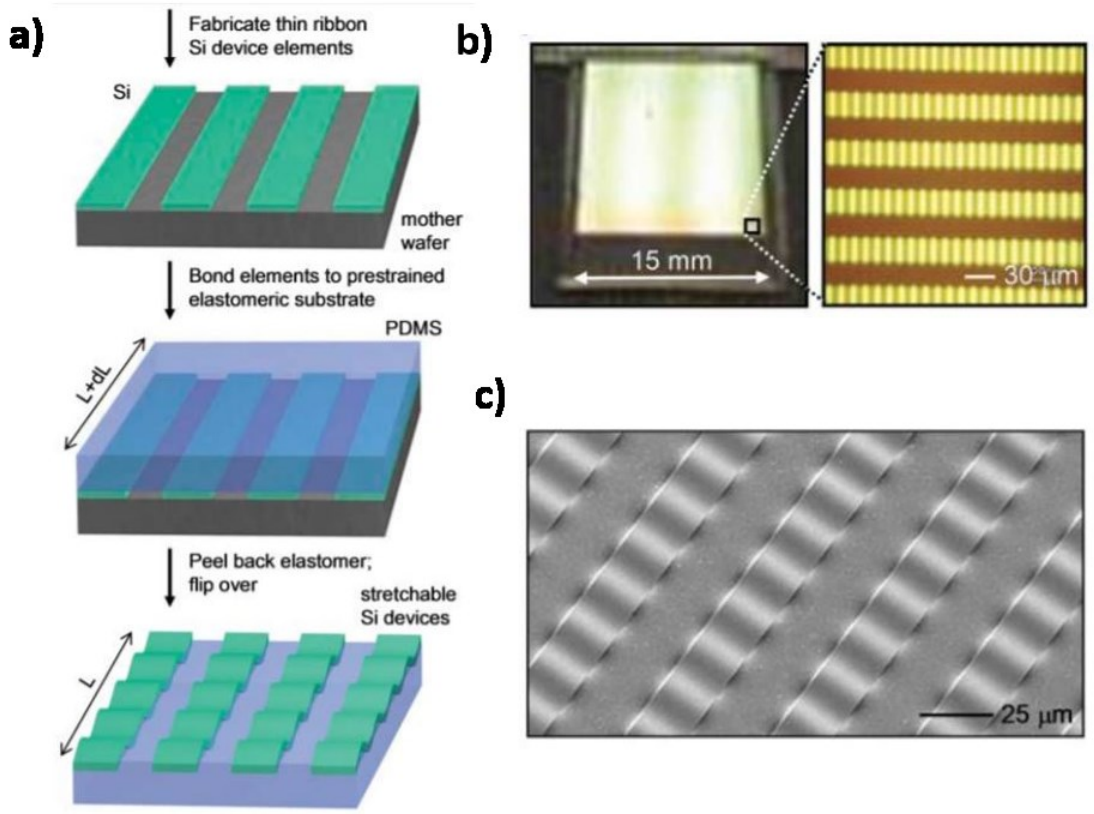

Figure1-1. [11] a) Schematic illustration of fabrication process for Si wrinkling thin film integrated with PDMS substrate. b) Optical image of a region of wavy patterns (widths= 20μm, spacing =20μm, thickness =100nm). c) Scanning electron microscopy image of four wavy Si ribbons with an angular view.

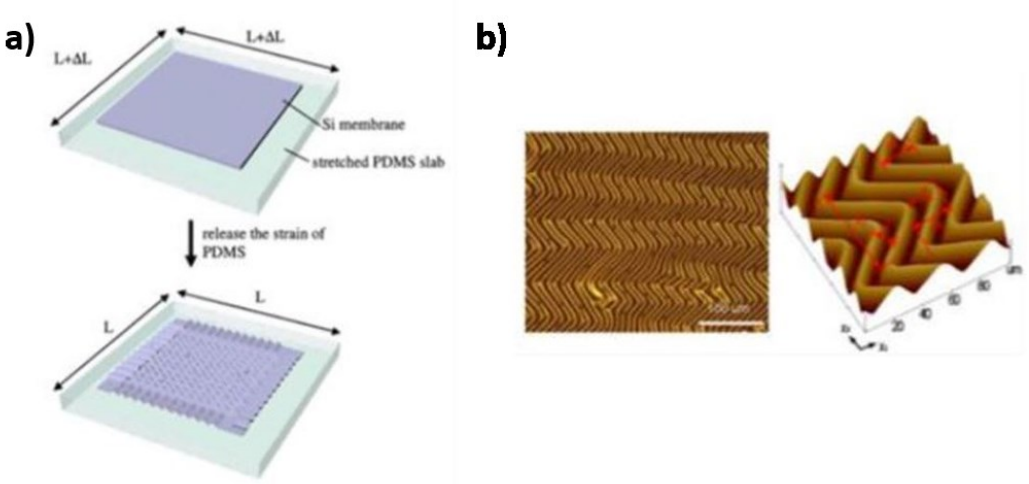

Figure 1-2 [25] a) Schematic illustration of the fabrication process of two-dimensional wrinkling patterns for Si membrane on PDMS substrate. b) Optical image of two-dimensional wrinkling region of Si membrane by optical microscope and atomic force microscope (AFM).

In addition, thermal mismatch is another milestone for fabrication of wrinkling pattern which is first proposed by Bowden et al. in 1998 [8]. In this study, the PDMS substrate bonded onto a glass foundation first to fix the bottom surface of PDMS substrate. Then, the top surface of PDMS expanded via introduced heating and at the meantime, a thin layer of Ti and Au deposited consecutively. Because the coefficient of thermal expansion of PDMS is much larger than that of top thin metal layer, after whole systems cooled down to room temperature, the wrinkling pattern were introduced by compression from soft substrate. Figure 1-3 b) shows the microscopy image of such two-dimensional surface morphology. Meanwhile, UVO and O2 Plasma combined with a specific pre-strain applied are also introduced to fabricate wrinkling surface morphology. Such method can avoid interfacial delamination or local defects with peeling off action which is possible for metal deposited-film-substrate system. By the way, its applicability in optical applications is better than metal deposited-film-substrate system since it will keep the initial transparency after surficial treatment.

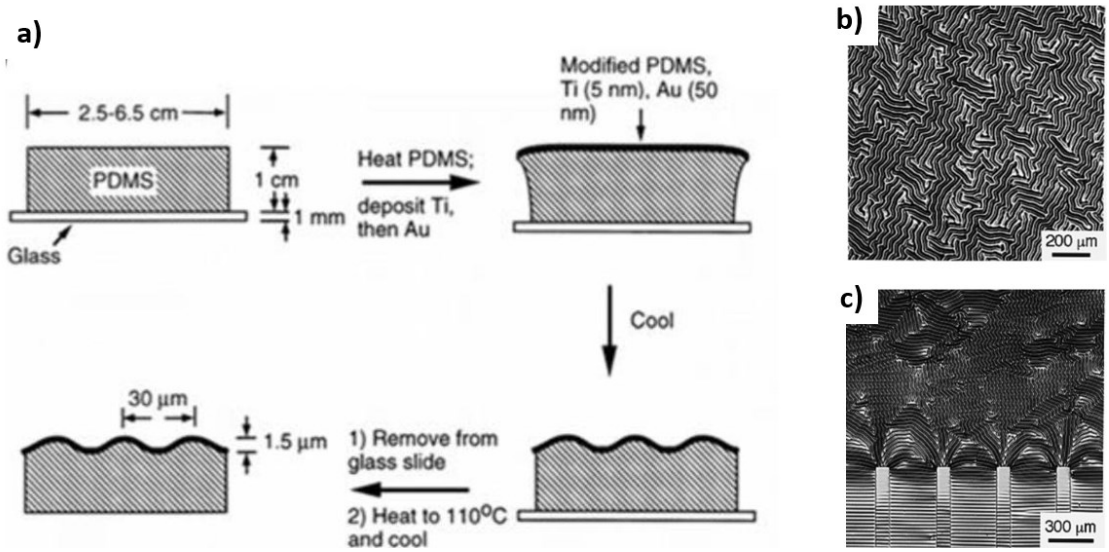

Figure1-3 [8] a) Schematic illustration of fabrication process for metal-film wavy pattern on soft PDMS substrate by thermal mismatch. b) The microscopy image of two-dimensional wavy patterns onto Au thin film. c) The microscopy image of transition state that one-dimensional wavy structure to two-dimensional state.

1.2. Surface Morphology-base optical systems

Thin-film wrinkles integrating with soft substrate promise several potential optical applications since the micro-scaled and nano-scaled surficial waves have different effects for transmitting light.

1.2.1 Optical Smart Window

Optical smart window with a tunable transmittance which can change from transparent to opaque state has attract lots of research interests for its potential benefits in power saving, indoor environmental adjustment and securing consideration [26-30]. However, the commercial smart windows suffer from high-cost batch manufacturing, unstable material with unpromising tunable recycles, multi-step fabrication process, and difficult

realization of actuation [31-35]. Micro-scaled structural array onto the soft substrate provides a bright future for smart window applications. Nowadays, several different surface-morphology-modified smart windows have been developed including quasi-amorphous array of silica nanoparticles (NPs) embedded in PDMS [36], nanopillar array onto wrinkled PDMS substrate [37], and wrinkled graphene-AgNWs hybrid electrode[38]. For example, Seung Goo Lee and his collaborators developed a new structure to tune the transparency and wetting of elastomeric [37]. Figure 1-4 (a) is the schematic illustration of such fabrication process. Nanopillar arrays first fabricated by micro-fabrication. And then the unpolymised PDMS is used to replicated the nanopillar arrays, then the UVO treatment is utilized while the pre-strain is applied. After releasing the strain, the tunable optical smart window has been accomplished. Figure 1-4(d) shows the optical image of such smart window switching reversibly from opaque (left) to transparent (right) circumstance (Pattern was fabricated by first UVO treatment).

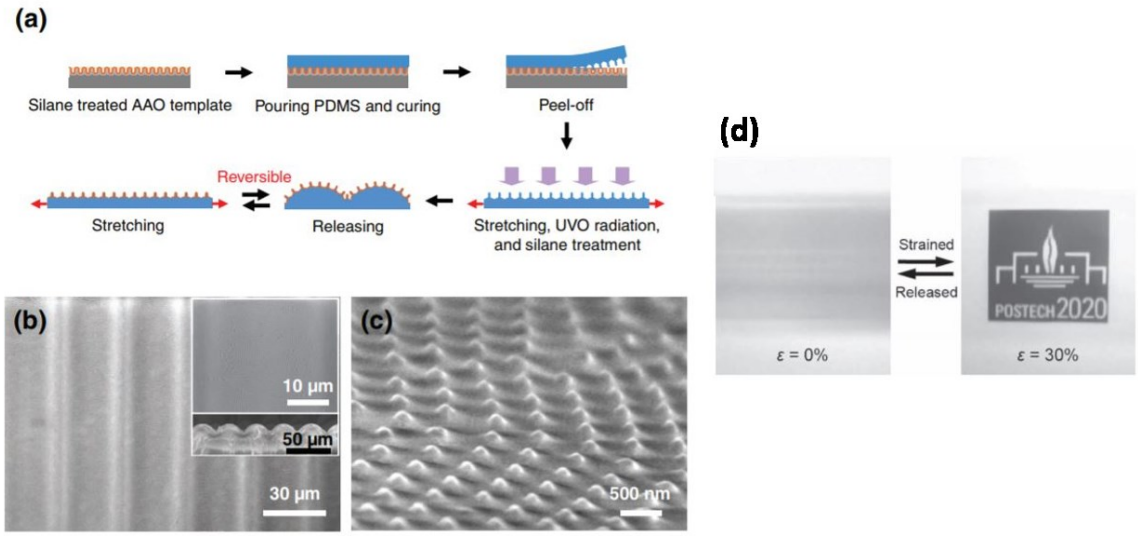

Figure 1-4 [37] (a) Schematic illustration of fabrication process of stretchable nanoplilar arrays onto the wavy PDMS substrate. (b) and (c) SEM image of nanopillar array on top of PDMS. (d) The reversible transmittance changes from transparent state to opaque state based on applied strain ε.

1.2.2 Optical diffuser

Optical diffusers are used to diffuse or soften the light for some potential applications. Optical diffuser has spread-out applications in liquid crystal display and LED illumination and display systems [39-42]. Liquid crystal display needs optical diffuser to be thermoduric, perdurable, and uniformly light distribution [43, 44]. On the other hand, for LED illumination, the softening, high transmittance and almost no diffraction phenomenon or diffraction patterns are overlapped with each other is preferable. Most optical diffusers can diffuser the light energy in Gaussian energy distribution and also shape the light beam by some novel structure design. Basically the light

diffuser can be classified into two categories. The one is grain-induced optical diffuser in which dense micro-scaled particles as diffusion components embedded into part of throughout the plastic substrate to diffuse the transmitting beam [45-49]. Second one is the surface-treated diffuser [50-55]. Normally, surface of plastic or elastic materials are treated with chemically etching, coating, or abrasion to generate a rough surface morphologies to diffuse the light. Figure 1-5 shows one type of optical diffuser fabricated by Takuya Ohzono in 2013 [55]. Figure 1-5 a) shows the experimental setup for the observation of diffusion laser spot. The wavelength of surface wrinkle here is about 4mm. And the distance from screen to wavy surface is fixed to 100mm. Figure 1-5 b) shows the diffusion patterns are differed from different s values which indicates different compression situations. Besides, the transmitting pathway is visible by introducing a mist as shown in Figure 1-5 c). When the two wrinkled surface which are both under compression is perpendicular to each other, the rectangular-shaped diffusion pattern can be obtained (shown in Figure1-5d). Another optical diffuser can be fabricated through silicone emulsions, the water drop distributed randomly as diffusion components after sufficient stirring. Figure 1-5e) is optical image of diffusers with different sized water drops randomly distributed within the silicone polymer. The digital image of blurred characters was also shown in Figure 1-5e). Figure 1-5f) shows different diffusion patterns when the laser beam went through with variable proportion of NaCl aq. solution.

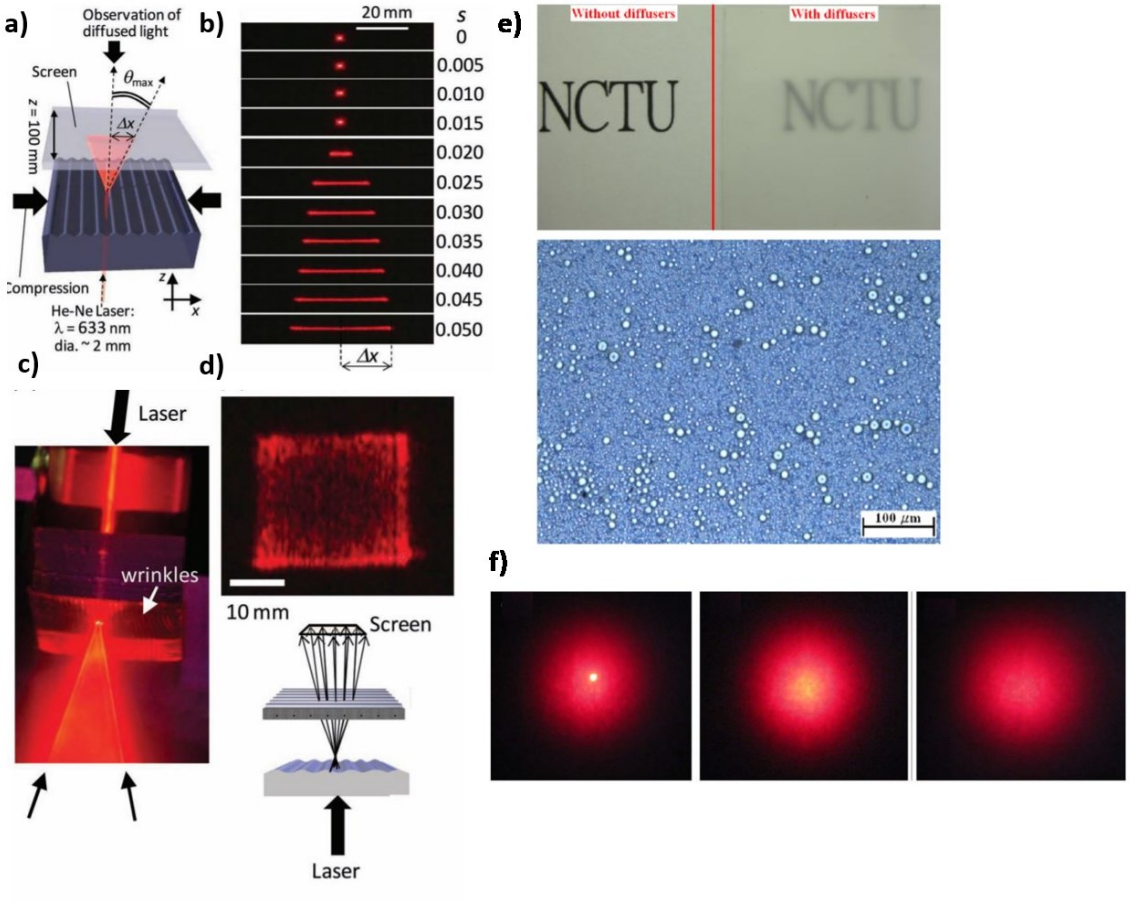

Figure1-5. [55] [56] Two types of optical diffusers. a) The experimental setup to observe the diffusive light. b) Digital photographs of laser diffusion patterns under different compressions. c) Visible diffused trace for laser beam. d) Rectangular-shaped diffusion pattern for two stacked samples. e) The diffusion effect for such optical diffuser to blur the character underneath and Optical microscopy image of such diffuser. f) The diffusion patterns for various vol% NaCl aq. solutions.

1.2.3 Optical grating

Optical grating is an important optical component with periodic, dense, paralleling structure which scatters and diffracts the light into several beams transmitting through different directions [59-62]. The optical grating utilizes multi-slit diffraction effect and light beam interference effect to scatter the transmitted light beam according to the wavelength [63]. Diffraction

phenomenon happens and dominates obviously when the size of narrow slit is comparable with the wavelength of transmitting light. The optical grating can be divided into two main categories. First is narrow-slit grating. Narrow-slit grating is line-shaped grating which realizes the diffraction effect by pinhole imaging theory. The high-performance diffraction pattern always implies low brightness and low transmittance. Another one is lenticular grating achieved by cambered lens imaging principle. The spectrum behind the optical grating always lines evenly and uniformly which induces its potential application in precise measurement. For example, the wrinkled film on soft substrates as tunable optical grating for strain sensing and measurement has been developed in 2013 [64]. The stretched PDMS substrate under uniaxial strain was deposited a layer of Au on top. After releasing the pre-strain, the evenly sub-micro-scaled wrinkled morphology generates at its top as shown in figure 1-5. Another high-performance TiO2-PDMS tunable optical grating has been fabricated by transfer printing technology as shown in Figure1 [65]. Figure 2 shows the low vacuum secondary electron image of TiO2 embedded into the soft PDMS substrate. The diffraction laser patterns are variable for different strains applied.

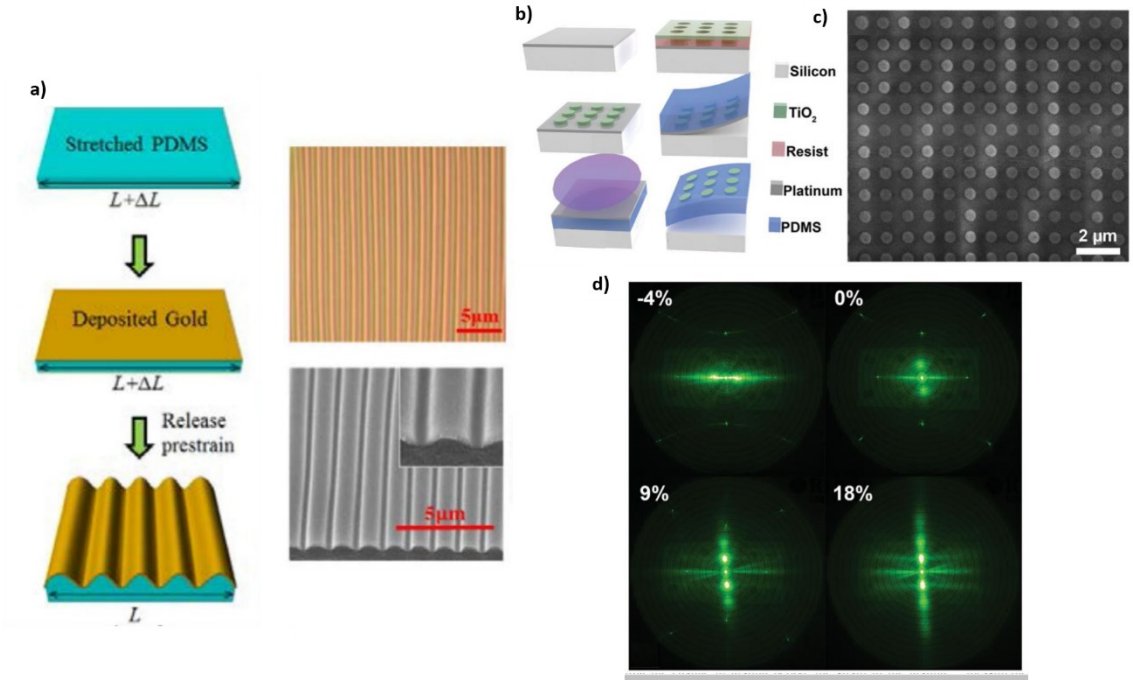

Figure 1-6. [64] [65] Two types of optical gratings: a) Schematic illustration of fabrication process for wrinkling Au film onto PDMS substrate for optical grating application and microscope picture of its wrinkling structure. b) Schematic illustration of preparation of TiO_2-PDMS tunable optical grating. c) Scanning electron microscopy (SEM) image of such optical grating's surface morphology. d) Tunable diffraction patterns of TiO_2-PDMS optical grating under different applied mechanical strains.

Chapter 2 Exploration of Tunable range of normal transmittance for smart window under various UVO treating time

2.1 Introduction

Nowadays, optical smart window whose light transmission properties can be adjusted has attracted a lot of interests due to its huge potential applications, such as automotive, aircraft, marine and architectural buildings in which smart window cannot only provide a comfortable indoor environment but also have far significance on low-carbon life. However, mass production of current available windows still have disadvantages such as high cost of manufacturing, and complicated assembled structure. Surface modification of soft active materials provide an opportunity for mechanically tuning light transmittance without affecting its intrinsic properties.

In this chapter, the tunable range of light transmittance has been explored under the foundational report by Zhengwei Li [66] where a cracking-wrinkling surface morphology is fabricated for smart window application. The optimal UVO etching time for cracking-wrinkling pattern which has best scattering effect has been demonstrated. The surface morphology is different under various UVO etching times. For 10mins UVO etched smart window sample, both micro-scaled wrinkling pattern and cracks cannot be observed; for 20mins, only cracks propagate perpendicular to uniaxial strain direction without the formation of wrinkling morphology. For 60mins, the optimal

transmission effect can be obtained where both cracks and wrinkles generate. And with increasing of UVO treating time. The top SiO_x layer is so thick that it is easy to facture with the strain applied. Therefore, the scattering effect will recede with further increasing UVO treat time.

2.2 Experimental Section

2.2.1 Preparation of various smart window samples

PDMS was prepared by homogenously mixing silicone elastomer and curing agent (Sylgard 184, Dow Coming) in a weight proportion of 10:1. The thorough mixture was then degassed in a vacuum desiccator for 40mins to remove all trapped air bubbles. After degassing, the mixture was placed in a flat platform with weight of 8g and was then cured in a hot oven at 80° for about 1hour. The polymerized PDMS film with thickness about 1mm was cut with 6cm*2cm strip for further surface treatment. The pre-stretched samples were then placed in a UVO cleaner (Jelight model 42) at a distance about 10mm for 20mins, 60mins, and 120mins respectively to generate a thin layer of SiOx on its top surface. Various surface morphologies can be obtained when a uniaxial strain was applied to different samples separately.

2.2.2 Characterization of morphologies

Optical microscopy images of various smart window samples were obtained by the optical microscope (BX60, Olympus) integrated with CCD camera in a

reflection mode. Scanning electron microscopy (SEM) were obtained by a Hitachi SU3500 microscope with an accelerating voltage of 30kV. Surface profiles for micro-leveled wrinkle were measured by Alpha-step 500 surface profilometer (Tencor). Crack depth of 20mins UVO etched smart window was checked by atomic force microscope (AFM) with tapping mode.

2.2.3 Optical Characterization

The normal transmittance of two samples stacking together was measured by the UV-VIS-NIR spectrophotometer (Shimadzu 3101PC). For the optical diffusive patterns, the light source was a collimated green beam with wavelength of 532nm transmitting through the optical diffuser sample. The white screen behind the sample was placed to collect and observe diffusive pattern. The distance from screen to sample was fixed to 43.5mm.

2.3 Results and discussion

Figure 2-1 a) shows the fabrication process of the PDMS films with different surface morphologies based on 20mins and 60mins ultraviolet/ozone (UVO) to etch freestanding PDMS film surface.[66] Here, UVO is used to oxidize the freestanding PDMS to generate a thin and rigid thin layer of SiOx. For the case which with 60mins UVO treatment, it will generate cracks along the vertical direction since the mechanical loading can easily exceed the critical cracking strain of the top brittle SiOx thin layer through the mechanical

stretching at two ends of treated PDMS film. The cracking along the vertical direction divide top thin layer into several micro-ribbons. When the mechanical stretching is large enough, due to Poisson's Effect, compression along the vertical direction will induce wrinkling at top surface of the PDMS film due to strain mismatch. However, for the case that with 20mins UVO etching, the mechanical stretching cannot exceed the critical stress corresponding to generation of vertical wrinkling patterns even if exceed 40% strain applied, only cracks are induced at top of surface. After the mechanical stretching is released, the film recovers to the initial flatten state (the series of wrinkling recovered to flatten and cracks become closed). Such phenomena reveals that the tunable transmittance range can be controlled by various UVO treating time since different UVO treating time will conduct various thickness of SiOx etched layer which will introduce different scaled patterns of wrinkles and cracks. The initial state of PDMS with 20mins& 60mins &120mins UVO etching are both transparent since the surface are both smooth and flatten (PDMS also has superior transparency, T% is about 90%), and after a specific mechanical stretching, the PDMS film with 60mins UVO treatment has become opaque comparing stretched PDMS film with 20mins UVO treatment (translucent), the characters "SMART WINDOW" is still visible underneath the stretched PDMS film with 20mins UVO treatment as shown in Figure 2-1 b). Further time UVO treatment case is discussed in later section.

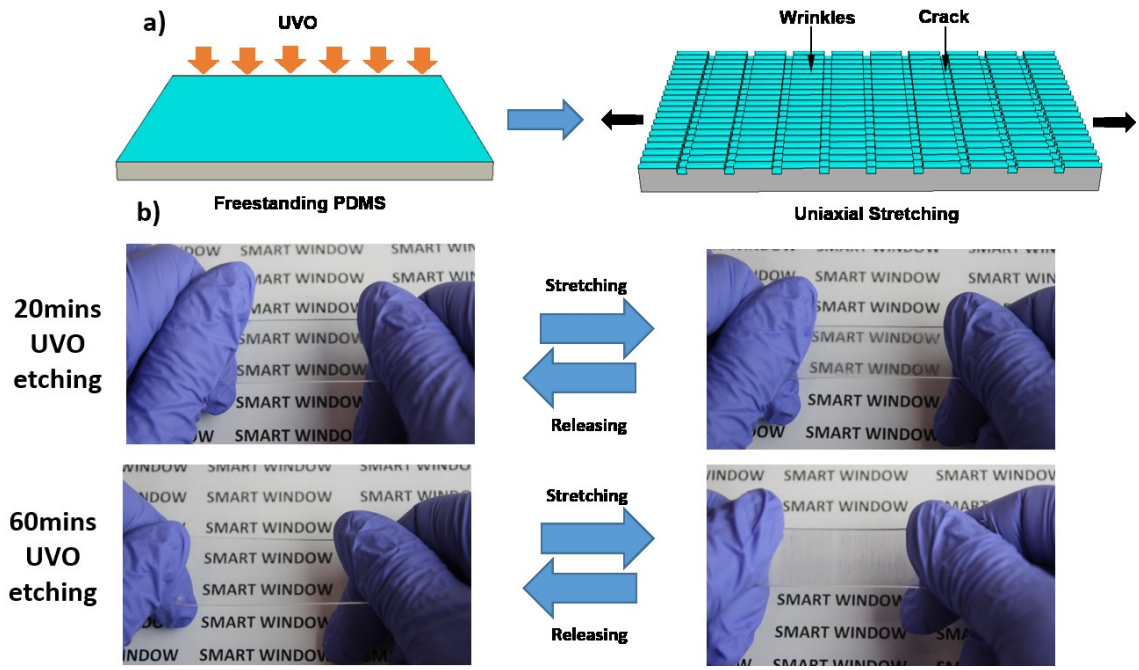

Figure 2-1 Fabrication process and switchable light transmission phenomena a) [66] Schematic illustration of preparation process for smart windows. b) Digital photograph to switch 20mins & 600mins smart window from transparent state to opaque/translucent state reversibly.

Figure 2-2 a) shows microscopy image of surface topography of 20mins & 60mins & 120mins UVO treatment with different mechanical stretching applied. The initial state of the PDMS film with 20mins&60mins&120mins all have a flattened no-cracked surface. When stretching applied, for example, 10% strain applied, cracks generate vertically at all three etched surfaces, due to the brittleness of SiOx layer and softness of PDMS substrate. The top SiOx layer is stretched into several ribbons divided by the microscale crack grooves. With increasing strain applied, wrinkling patterns initialized first for 120mins UVO treated sample when strain reached 10%. That's because it has thickest oxidized layer with largest local stress mismatch and lowest critical strain for wrinkling pattern generation. Then when applied

strain reaches 20% for 60mins, the applied strain has reached the critical buckling strain of thin film-substrate system (stiff SiOx layer on soft PDMS substrate), wrinkles start to form along the vertical direction. When applied strain increased to 30%, for 60mins&120mins UVO treated samples, wrinkling patterns fully developed onto the cracked surface respectively. For 20mins UVO treated PDMS, the cracks becomes more dense but without wrinkling pattern generated even if the applied strain exceed 50%. For 60mins& 120mins UVO etched PDMS film, the surface wrinkling-cracking becomes much denser with increasing applied strain. However, the applied strain can only reach to 30% for 120mins UVO treated sample since the PDMS film will be raptured with further increased strain. This phenomenon is due to the increasing depth for cracking grooves, and the treated surface is much thicker and brittle with long-time UVO etching. As shown in figure, the depth of cracking reach about 7um which means the cracks is much easier to propagate. As the etching time reduced, the depth of cracking reduced for different treated samples. Because the top SiOx layer is so brittle that the stress needed to fracture such layer which means the crack is easy to formulate. With the increased normal stress or increased normal stress, the cracking region has larger potential to propagate, and with deeper cracks, it much more easy to fracture. The figure 2 show the depth of cracks under different UVO etching time obtained by profilometer (Alpha-Step D-500, KLA-Tencor.). The normal strain for PDMS films are all 30%. Besides, the

fracture of angle for is increasing with the UVO etching time which also supported by fracture theory. The relationship between wavelength, amplitude and applied strain is shown in Figure 2-2b) for different cases. With the increasing applied strain, the wavelength is decreasing and amplitude is increasing. The relationship between wrinkle wavelength/amplitude can be described by a finite deformation model for buckled film on a compliant support [66].

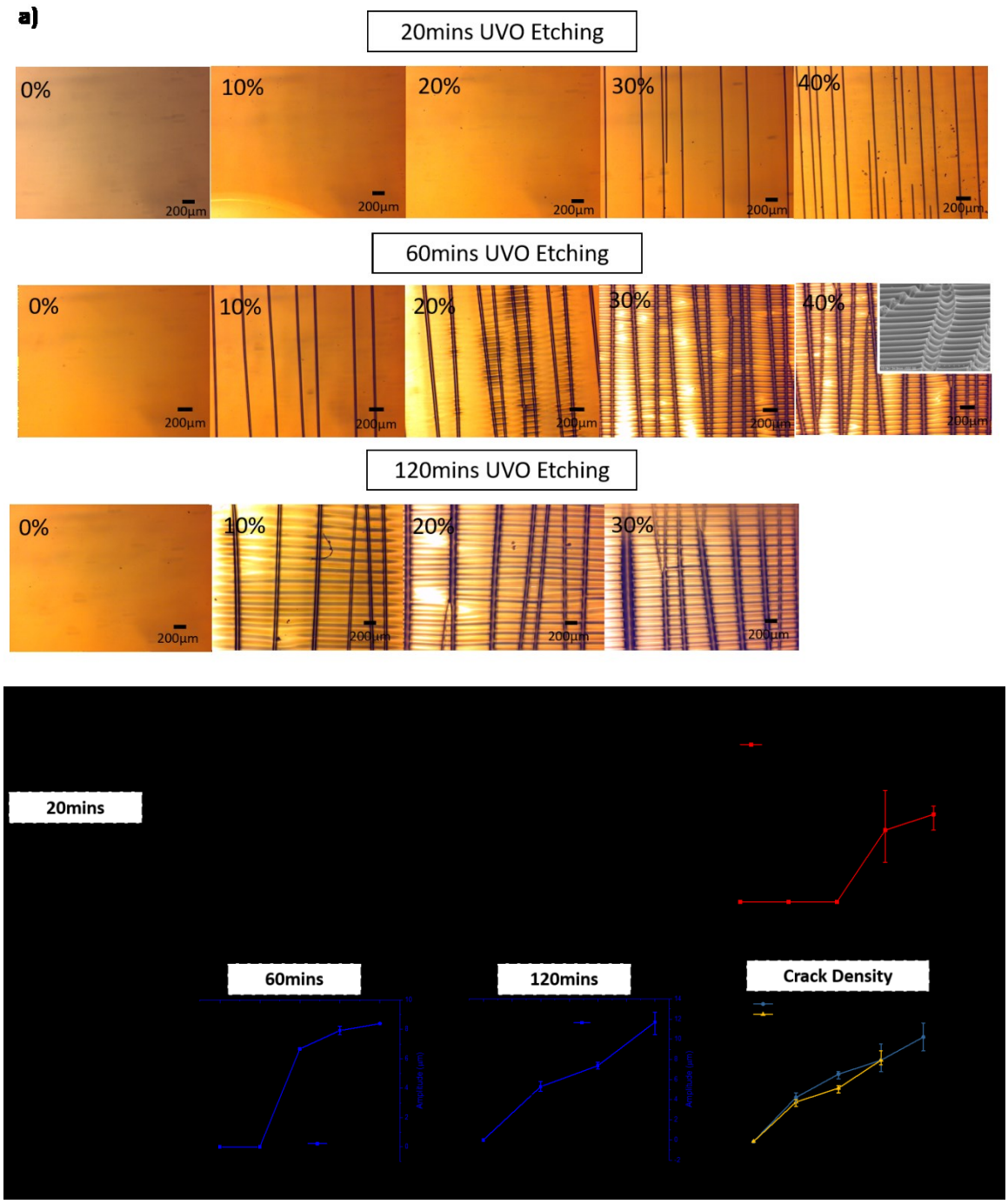

Figure 2-2 Surface morphologies and profiles for 20mins, 60mins, and 120mins UVO etched samples. a) Optical microscopy images of 20mins, 60mins, and 120misn UVO etched smart windows (Scaled bar: 200μm) The insert image shows SEM image from a tilt view for 60mins smart window under 40% strain applied. b) Surface profiles for 20mins, 60mins, and 120mins UVO treated samples, b)i Surface profile for 20mins sample along vertical direction; ii Surface profile for 20mins sample along horizontal direction under 40% strain applied; iii The crack density per millimeter versus applied strain for 20mins sample; iv The relationship between wavelength and

amplitude of surface wrinkling patterns for 60mins UVO treated sample, the inserts are horizontal and vertical direction profiles under40% strain applied; v The relationship between wavelength and amplitude of surface wrinkling patterns for 120mins UVO treated sample, the inserts are horizontal and vertical direction profiles under 30% strain applied; vi The crack density per millimeter versus applied strain for 60mins sample and 120mins sample.

The combined wrinkling-cracking surficial morphologies provides a meaningful approach for scattering and diffusing the light when light passes through the surficial morphology. The sample is transparent for 20mins/60mins/120mins UVO treated sample with no strain applied. As a 10% strain is applied, the transparency decreases due to the appearance of surficial cracking for 60mins PDMS film. For 20mins case, the transparency keeps its initial transparent state due to no structural change. And due to the large-area wrinkling pattern formation, the characters underneath the 120mins UVO treated sample is hardly to see compared with 20mins/60mins sample with identical strain applied. For the different UVO timely treated sample, the critical strain corresponding to completely opaque sample is different. For the 20mins UVO etched PDMS film, when the strain reaches out 50%, the characters underneath the sample is still clear since no wrinkle at horizontal direction formed. For the 60mins UVO etched PDMS film, when 40% strain is applied, the sample has become completely opaque. For the 120mins UVO etched PDMS film, only 30% strain applied is a limitation for the opaque surface due to the experimental results, when the applied strain reached out more than 30%, the PDMS film is easy to fracture. Moreover, the optical diffusive image for different surficial structure can also demonstrate

such issue. For 20mins sample, the optical diffusion pattern is only a light line along horizontal direction due to its vertical-aligned cracking pattern. For 60mins/120mins sample, with the wrinkling patterns combined with surficial cracking, the horizontal light line has been diffused at vertical direction by the wrinkling patterns which means the wrinkling surficial structure has a scattering effect for a light source. Furthermore, A Cary 5000i UV-vi-NIR spectrophotometer is then used to measure the normal transmittance for time-different UVO etched PDMS films. The relationship between applied strain and an average normal transmittance from wavelength 380nm to 780nm (visible light region) is shown at figure. For the 20mins UVO etched PDMS film, the normal transmittance is decreasing not much with increasing applied strain. Within the region from 0% applied strain to 20%, the normal transmittance remains a constant since there is no large-area cracking patterns initiate. From 20% applied strain to 40%, normal transmittance dropped but not too much from 92.5% to 78.2%. For the 60mins/120mins UVO etched PDMS film, the normal transmittance dropped dramatically from about 90% to below 20%. Both 60mins% 120mins UVO treated sample's normal transmittance show two stages: (1) at 0%-20% strain level, the normal transmittance changed dramatically because strong light diffusive effect by wrinkling-cracking surficial structures. (2) after 20% level, the large-area wrinkling cracking patterns has formed, the normal transmittance generated placid, which means minimal light transmittance

can be reached by mechanical stretching. The curve for 60mins UVO etched sample is always underneath the curve for 120mins UVO etched sample which represented there is optimal UVO etching time for PDMS film since with the increasing amplitude for 120mins sample compared with 60mins sample, the wavelength is larger as well which can be explained by which the wrinkling surface for 60mins is steeper than other kinds of samples which means the scattering effect for 60mins UVO etching sample is optimal. The normal transmittance cannot keep reducing since the applied go beyond 30%, it will go instable to fracture. Therefore, we can obtain the tunable range of normal transmittance via different UVO treatment time. And basically, the wrinkling patterns dominate the diffusion phenomenon compared to contribute of crack grooves.

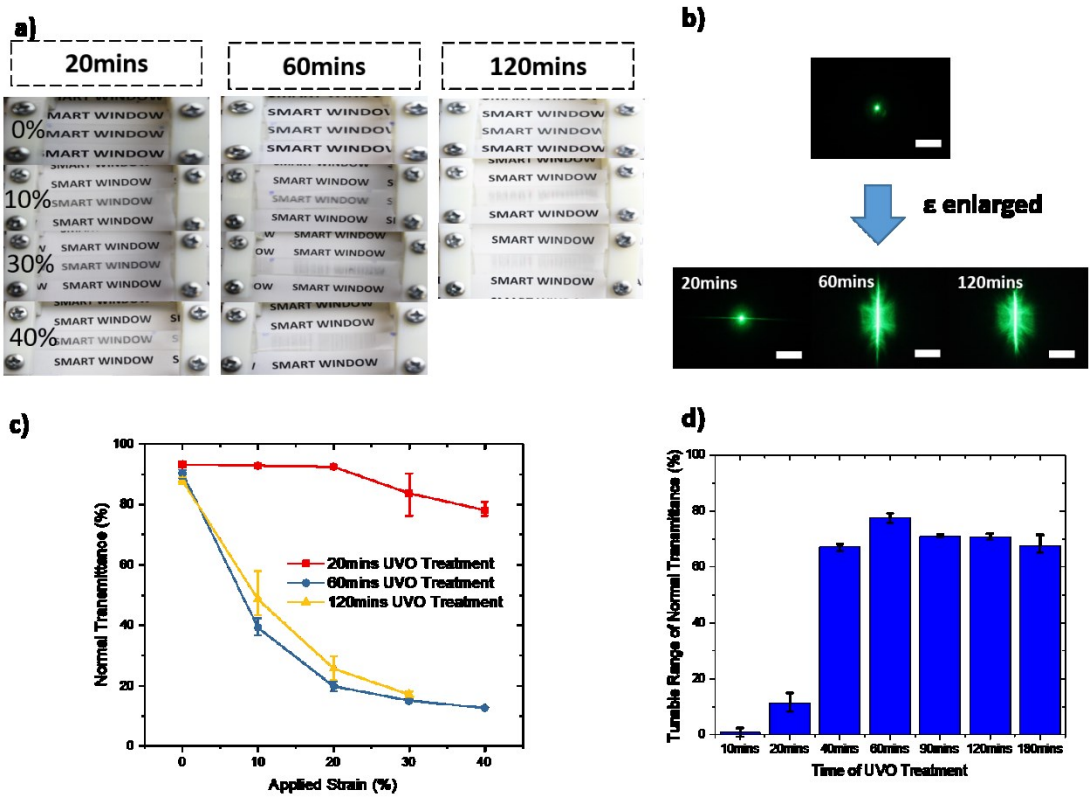

Figure 2-3 Optical performance for various optical smart windows. a) Digital photographs of various smart windows under various applied strains. b) The diffusion optical patterns for various smart windows when a green light beam (wavelength: 532nm) passes through. c) The relationship between the normal transmittance versus various applied strains for different smear window samples. d) The tunable range of normal transmittance for different smart windows.

UVO Etching Time (mins)	20mins	60mins	120mins
Wrinkle Wavelength (μm)	---	~87	~140
Wrinkle Amplitude (μm)	---	~8	~12
Crack Density (mm^{-1})	11	16	12
Crack Depth (μm)	0.5~1	10~20	More than 40
Minimum T%	~80	~10	~20
Tunable Range (%)	~15	~80	~65

Table 2-1. Complex comparison between 20mins&60mins&120mins UVO etched smart window samples.

2.4 Conclusions

In summary, the optimal UVO etching time (60mins) for cracking-wrinkling pattern which has best scattering effect and tunable range of normal transmittance for various UVO treated smart windows have been demonstrated. The optimal tunable transmittance range is about 80% which is higher-performance than the state-of-the-art optical smart windows. Our optical window can also switch from transparent state to opaque reversibly. Such study and exploration has a huge impact not only on smart window applications but also on the optical devices which needs switchable optical components for specific utilization.

Chapter 3 Tunable Screwthread-like Wrinkling Patterns for Optical Diffuser Applications

3.1 Introduction

In this paper, we represent a simple and cheap approach via surficial wrinkling pattern and PDMS molding replication to fabricate a tunable high-performance optical diffuser based on two-dimensional micro scaled screwthread-like wrinkling patterns. Well-proportioned quadrate-shaped diffusion patterns can be obtained when a collimated light beam transmits through our optical diffuser. To further upgrade our light properties, we fabricated two-sided rough surficial morphology-based optical diffuser with increasing light scattering angle, larger scattering region and optical haze transmittance. Furthermore, the two-dimensional surficial structure can be tune to one-dimensional wrinkling pattern though easy mechanical stretching. Such reversible process can be used to tune the diffusion patterns from a squared shape to a narrow strip by simple mechanical actuation [67]. (This work was finished by the collaboration of Dr. Zhengwei Li and Yinding Chi)

3.2 Experimental characterization

3.2.1 Sample preparation

PDMS was prepared by homogenously mixing silicone elastomer and curing agent (Sylgard 184, Dow Coming) in a weight proportion of 10:1. The

thorough mixture was then degassed in a vacuum desiccator for 40mins to remove all trapped air bubbles. After degassing, the mixture was placed in a flat platform with weight of 8g and was then cured in a hot oven at 80 for about 1hour. The polymerized PDMS films with thickness about 1mm were cut with a wideness 3cm strip for further surface treatment. The PDMS samples were then fixed with a uniaxial prestrain 20% by a hand-made stretching step. The pre-stretched sample was then placed in a UVO cleaner (Jelight model 42) at a distance about10mm for 60mins to generate a thin layer of SiOx on its top surface. One-dimensional wrinkling pattern generate spontaneously at stretching direction after the stretching released. Three identical samples aligned together for next-step mold. The thoroughly degassed but uncured PDMS mixture was then poured over three aligned wrinkling surface and cured at 80° for 1 hour. After cooling to room temperature, with peeling off from the templated carefully, the PDMS replica with one-dimensional wrinkling surficial pattern are obtained. The replica was then cut and pre-stretched to 20% perpendicular to first wrinkling direction and then placed in the UVO cleaner for 1 hour following same step for first wrinkling pattern fabrication. After releasing the 20% strain, the screwthread-like wrinkling surficial pattern was obtained for potential optical diffuser application.

3.2.2 Structural Characterization

Optical microscopy image of optical diffuser was obtained by the optical microscope (BX60, Olympus) integrated with CCD camera in a reflection mode. Scanning electron microscopy (SEM) image was obtained by a Hitachi SU3500 microscope with an accelerating voltage of 30kV. Surface profiles for two-dimensional srewthread-liked wrinkling patterns were measured by Alpha-step 500 surface profilometer (Tencor) (Same steps for all other stretched states).

3.2.3 Optical Characterization

Total and diffusive transmittance of optical diffuser under various strains was measured by the UV-VIS-NIR spectrophotometer (Shimadzu 3101PC) integrated with integrating sphere (Shimadzu ISR 3100). The haze transmittance was generated by the ratio of diffusive transmittance versus total transmittance. For the optical diffusive patterns, the light source was a collimated green beam with wavelength of 532nm transmitting through the optical diffuser sample. The white screen behind the sample was placed to collect and observe diffusive pattern. The distance from screen to sample was fixed to 43.5mm. Diffusive transmittance: the amount of light transmit beyond a central angle of 24°; Total transmittance: the amount of light transmit our optical diffuser sample.

3.3 Fabrication Process

Figure3-1 schematically represents the fabrication process of optical diffuser sample. The UVO treatment is first introduced to generate a thin layer of SiOx at top surface of a uniaxially pre-stretched PDMS film. After releasing the strain, the wrinkling pattern generated spontaneously since the mismatch of mechanical properties between SiOx thin layer and PDMS substrate. The wavy PDMS film can work as a template for following molding replication. The uncured PDMS mixture was poured over the wrinkling template. After peeling off from the template carefully, the PDMS polymer replicated the original surface patterns perfectly due to its low surface energy. The replica was then stretched perpendicular to first wrinkling direction. After the second UVO etching, the screwthread-liked surficial patterns can be obtained for potential optical diffuser.

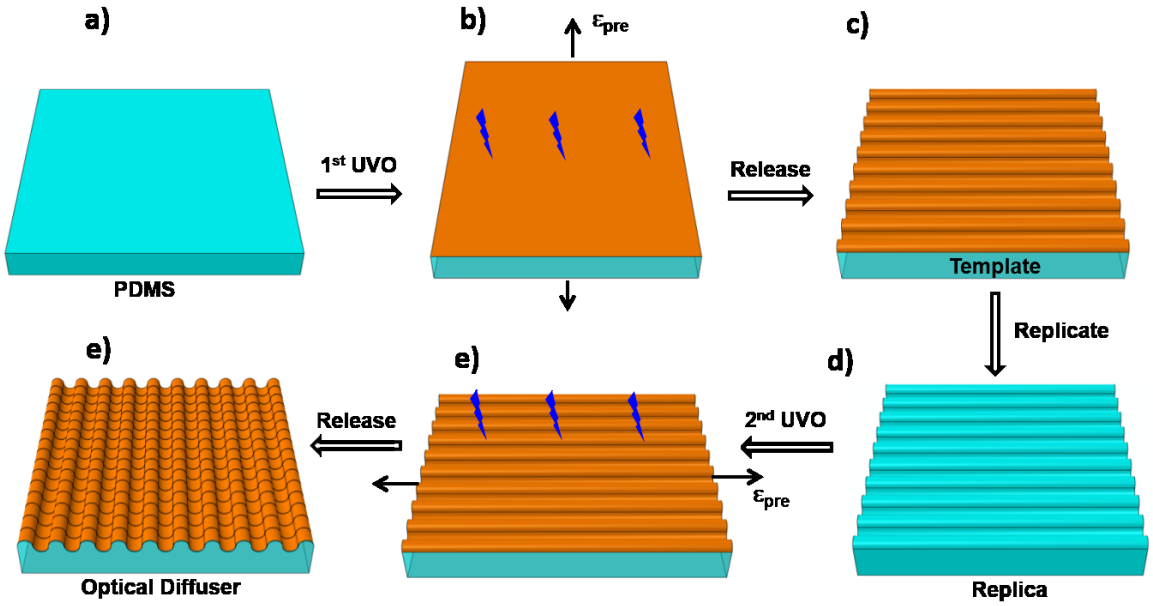

Figure 3-1. Schematic illustration of fabrication process for tunable optical diffuser. a) Freestanding pure PDMS substrate. b) Pre-strain applied to PDMS with UVO treatment. c) After releasing the strain, uniform wrinkling patterns formed. d) Another uncured PDMS as a replica to replicate wavy surface morphology. e) Second UVO treatment to PDMS replica with a pre-strain applied perpendicular to first strain. f) After second strain releasing, the screwthread-like surface morphology formed.

3.4 Surface Morphology Analysis

Surficial morphology of PDMS film is shown in figure 3-2 a). From the microscopy image of surficial pattern, uniform large-area micro-scaled square-liked structure can be observed. With the identical 20% prestrian applied horizontally and vertically, the rectangular but not square units array generate. The reason for this, on the one hand, is that the first replicated wrinkling is under compression due to Poisson's Effect at vertical

direction when a horizontal directional stretching applied to generate second wrinkling patterns. After the UVO etching and releasing the strain, the wrinkling patterns cannot recover to its initial state due to its changed mechanical properties (The surficial thin layer is much rigid than PDMS substrate). On the other hand, first replicated wrinkling surface morphology affect local stress distribution and thickness of TiOx layer. Therefore, the wrinkling unit is a rectangular shape other than square shape. Figure3-2b) shows the SEM image of wrinkling surface from a tilt angle which clearly verified the screw-liked surficial structure. The second propagated wrinkling patterns were along horizontal direction and first replicated wrinkling pattern was the “arches” between wrinkling patterns adjacent.

Figure 3-2 c) and d) shows the scanning profile of surficial wrinkling patterns horizontally and vertically. The wrinkling patterns from each direction propagate uniformly. The average wavelength and amplitude for horizontal direction are 103.7um and 6.7um respectively. The average wavelength and amplitude for vertical direction are 60.6um and 0.95 um respectively. The horizontal profile is much larger than vertical profile which also demonstrate the small unit is rectangular shape other than square shape.

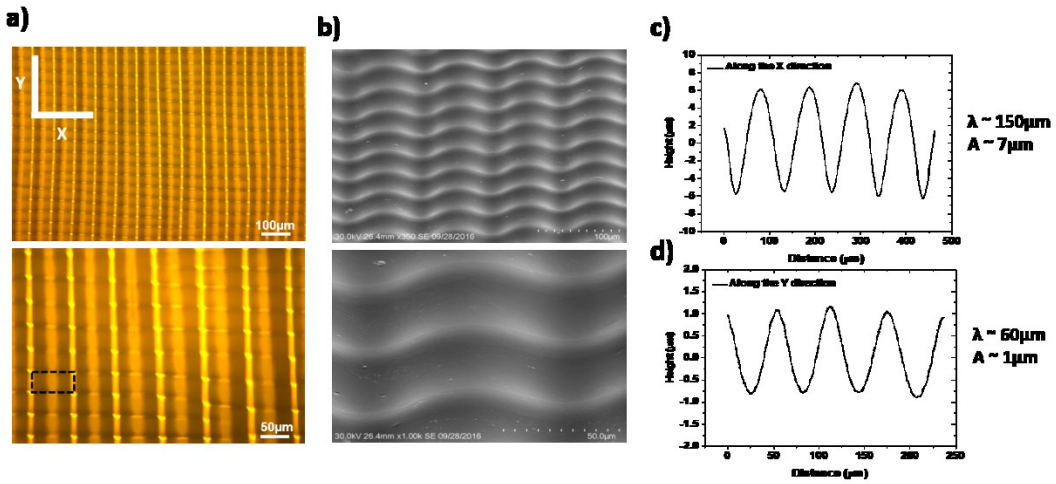

Figure 3-2 Surface morphology and profiles for screwthread-liked structure. a) Microscopy image of large region of rectangular units arranged uniformly. b) Scanning electron microscope (SEM) image of micro-structure from a titled view. c) Surface profile for optical diffuser along horizontal direction. d) Surface profile for optical diffuser along vertical direction.

3.5 Optical Properties Analysis

After the investigation of its surface morphology, the diffusive optical patterns are studied when the collimated light source went through the optical diffuser. The distance between the rough surface of sample and the detected screen is fixed to be 43.5mm. Figure 3-3 a) shows the rectangular shaped optical patterns for one-sided optical diffuser. Both top and bottom shrined a little bit from our observation since the second prestretching for the PDMS film introduce the compression at vertical direction due to the Poisson's Effect, the horizontal direction cannot rebound to its initial state since the rigid SiOx layer exhibited by 1hour UVO etching. Figure 3-3 b) shows the magnified rectangular shaped optical patterns for two-sided optical diffuser since two roughed wrinkling surfaces have better light scattering

effect. More to the point, the light intensity for one-sided and two-sided samples can be obtained via ImageJ processing. From figure 3-3c, the uniformly distributed light intensity can be obtained horizontally and vertically respectively. The broader scattering region at X direction than Y direction can be explained by the larger wavelength at horizontal direction compared with vertical profile. Figure 3-3 d shows that the light intensity distribution region for two-sided sample is much larger than one-sided situation. That's because two rough surfaces scattered the light source twice.

High diffusive transmittance and Haze index are two important indicators for optical diffuser evaluation. To quantitively measure these optical properties of our optical diffusers, a UV-vis –NIR spectrophotometer with integrating sphere was utilized. The experimental results show that the total transmittance has reached about 85% for both one-sided and two sided sample (most of the light went through PDMS film without reflection and absorption), but the diffusive transmittance for two-sided sample is about 65% which is much larger than one-sided ~45% diffusive transmittance. With the proportion between the total transmittance and diffusive transmittance, the Haze index can be set up in Figure 3-3f). The haze transmittance for two-sided sample reached about 80% which is more than 20% higher than one-sided optical diffuser. The reason is that the collimated light source reflecting& refracting at both two rough surfaces so that the scattering rectangular region for two-sided sample is much larger than one-sided.

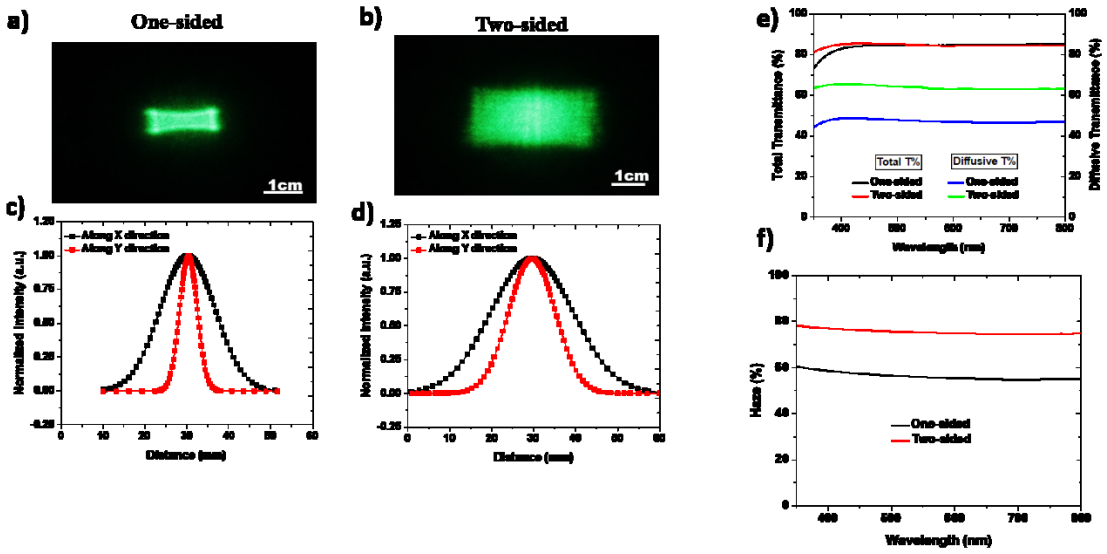

Figure 3-3 Optical performance for one-sided and two-sided optical diffusers. a) The digital image of one-sided optical diffusion pattern. b) The digital image of two-sided optical diffusion pattern. c) The normalized light intensity for one-sided optical diffuser along X and Y directions. d) The normalized light intensity for two-sided optical diffuser along X and Y directions. e) Diffusive and total transmittance from wavelength 300nm to 800nm fir both one-sided and two-sided optical diffusers. f) The Haze index for both one-sided and two-sided optical diffusers.

3.6 Deformable surface morphology

Another novel feature for our screwthread-like microstructure is that the surficial two-dimensional wrinkling patterns can be tuned to one-dimensional due to simple mechanical actuation shown in Figure 3-4a. With the increased applied strain from 0% to 20%, the second generated wrinkling at horizontal direction become flatten gradually, and the first replicated wrinkling become more obvious. When the applied strain reached to 20% which is same with the second pre-strain, the surficial pattern almost recover to its initial stage without second UVO etching and pre-strain. Then the quantitative analysis for tunable surficial profiles were studied by using the profilelometer, the

quantitative surficial diversification versus applied strain is obtained from Figure 3-4 b) &c). Along the x direction, the amplitude decrease rapidly from about 7um to 1um with the x-directional stretching. On the other hand, the wavelength increase from ~90um to ~115um. The horizontal wrinkling cannot be perfectly stretched to flatten since the existence of cracks along the vertical direction will release the strain when stretching introduced. And along the y direction, since the stretching introduced at x direction would induced the compression due to Poisson's Effect at another direction, the amplitude increased dramatically in the meantime wavelength decreased when increasing applied strain applied. It's a robust and reversible process changing from two-dimensional structure to one-dimensional structure without any structural violation. The optical properties such as transmittance will be discussed in next section.

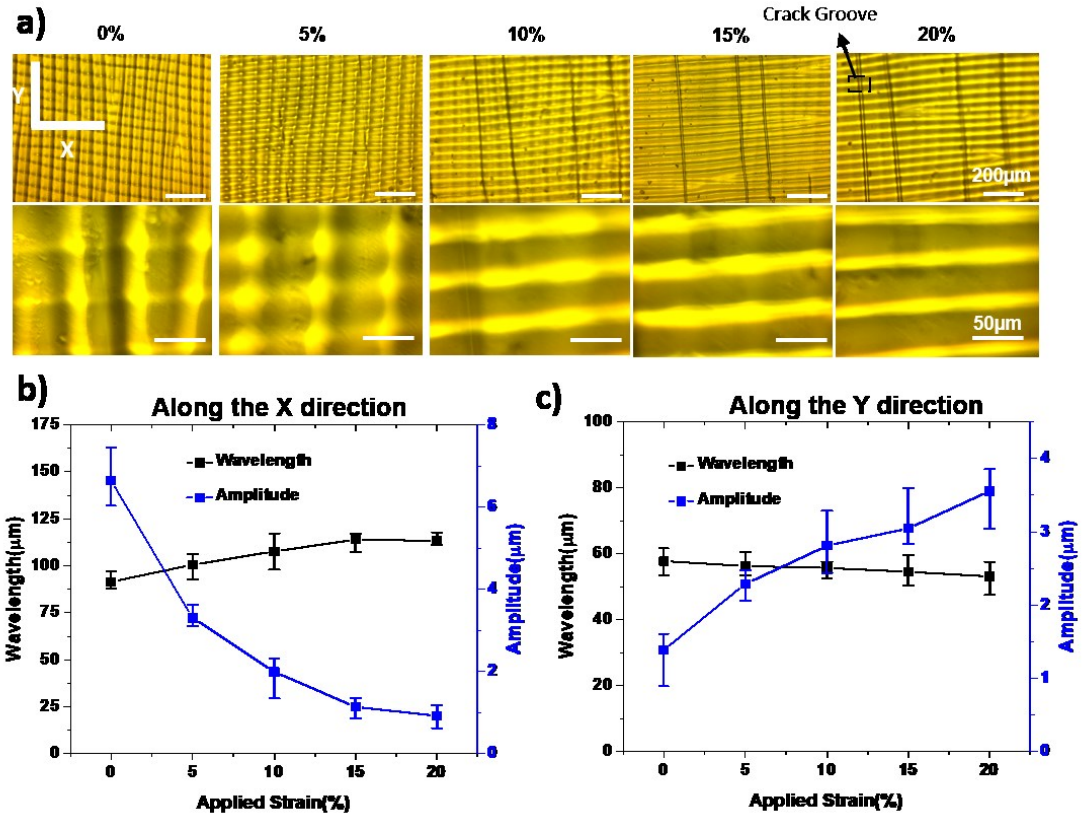

Figure 3-4 Deformable surface morphology and profiles for one-sided optical diffuser. a) Microscopy image of surface morphology changed from two-dimensional to one-dimensional under the increasing strain applied. b) The relationship between wavelength and amplitude versus increasing applied strain along the horizontal direction. c) The relationship between wavelength and amplitude versus increasing applied strain along the vertical direction.

3.7 Tunable Optical Diffuser

With the development of photonics and optoelectronics, the optical component needs to be tunable with an easy actuation which allows real-time monitoring and environmental flexibility. Various structural morphologies induce various optical diffusive patterns, therefore for our optical diffuser the tunable surficial morphologies can be used for tunable optical patterns when a light source transmits through. From the Figure 3-5 a) the optical light

spots versus increased applied strain was shown. The original rectangular shaped light region shrinks along the horizontal direction to a narrow light stripe both for one-sided and two-sided samples as applied strain increase from 0% to 20%. The light spots shrinks along horizontal direction can be explained by horizontal wrinkling patterns become flatten. In addition, the light spots elongate along vertical direction since the combination of more inclined wrinkling pattern and cracks along the vertical direction were introduced. Then the relationship between the scattering angles and the applied strain can be obtained in Figure 3-5c) and d). Take one-sided sample as example, the scattering angle along the x direction changed from 30° to 10° since the subdued horizontal wrinkles while scattering angle increase along y direction especially from 10% to the 20% with a dramatically increasing slope which is because not only the increased aspect ratio for wrinkling patterns along the transverse direction but also the narrow cracking grooves along the transverse direction has been expanded. All in all, from the optical analysis in figure 3-5, our tunable surficial wrinkling pattern can be utilized for potential tunable optical diffuser applications. The optical photographs and optical properties can be tuned by a dynamically straightforward actuation.

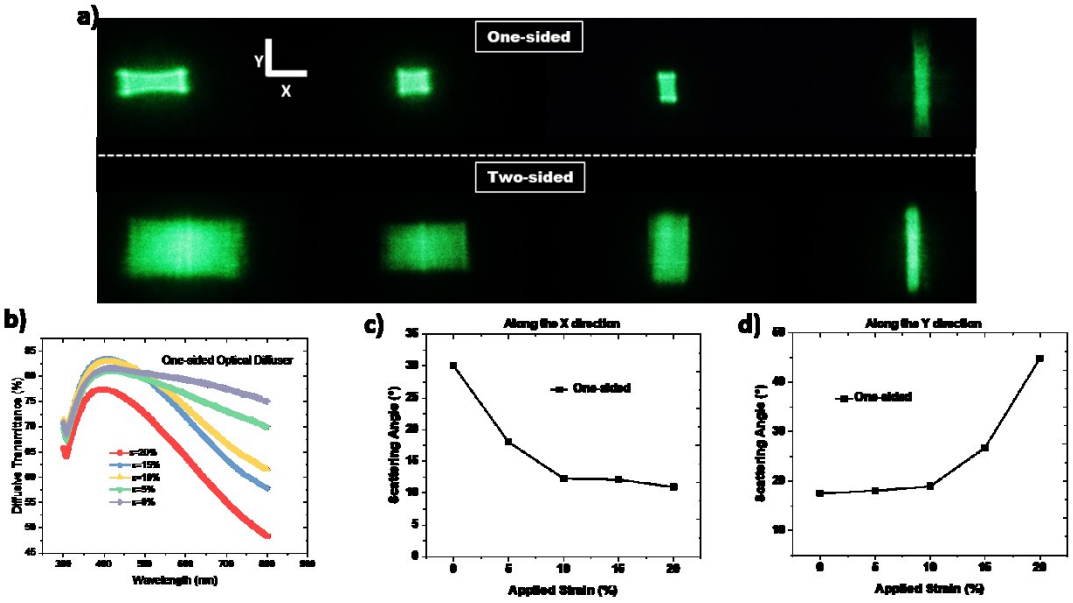

Figure 3-5 The tunable optical performance for both one-sided and two-sided optical diffusers. a) The deformable diffusion from rectangular shape to a stretched line shape with increasing uniaxial strain for both one-sided and two-sided optical diffusers. b) The diffusive transmittance for one-sided optical diffuser under various strain applied. c) Variation of scattering angle versus applied strain for one-sided optical diffuser. d) Variation of scattering angle versus applied strain for one-sided optical diffuser. The distance from the screen to optical diffuser is to be fixed to 43.5mm.

3.8 Supplement

By changing the angle for propagation directions between two one-dimensional wrinkles when second strain applied, some novel diffusion region can be obtained as shown in Figure 3-6 b). The second propagation direction has 45° angle with the vertical propagated wrinkles when a ∠45° directional pre-strain applied to PDMS replica. Figure 3-6 a) shows the microscopy image of uniform arranged wrinkling structures. The quasi parallelogram-shaped diffusion can also be obtained when the light beam transmit through for special optical applications.

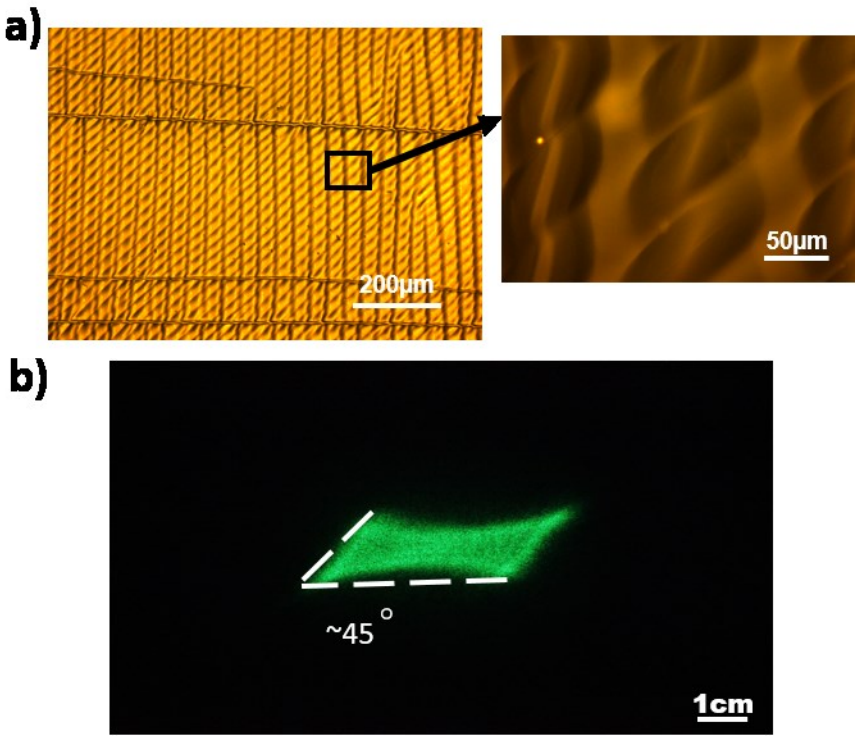

Figure 3-6. Preparation of ∠45° optical diffuser. a) Microscopy image of 45° screwthread-liked morphology. 2) Digital image of parallelogram-shaped diffusion region.

3.9 Conclusions

In this chapter, a simple, cheap and high-effective approach is introduced to fabricate a high-performance optical diffuser by combination of wrinkling patterns and molding replication to generate a micro-scaled two-dimensional surface morphology. Such optical diffuser can uniformly diffuse light spot into a rectangular shaped region, which has a high optical performance like diffusive transmittance and haze index. Furthermore, a two-sided screwthread-liked optical diffuser is proposed to enhance the optical performance in diffusion and scattering region. With deeper analysis of surficial morphology, another unique feature for our optical diffuser is that

its two-dimensional screwthread-like surface structure can be easily tuned to an on-dimensional wrinkling structure via simple mechanical stimulation, which indicates its variability in optical performance such as scattering angle.

Chapter 4 Harness Two-layer Hierarchical Surface for Deformable Optical Grating

4.1 Experiment Section

4.1.1 Sample Preparation

PDMS was prepared by homogenously mixing silicone elastomer and curing agent (Sylgard 184, Dow Coming) in a weight proportion of 10:1. The thorough mixture was then degassed in a vacuum desiccator for 40mins to remove all trapped air bubbles. After degassing, the mixture was placed in a flat platform with weight of 8g and was then cured in a hot oven at 80° for about 1hour. The polymerized PDMS films with thickness about 1mm were cut with 6cm*2cm strip for further surface treatment. The PDMS samples were then fixed with a uniaxial pre-strain 20% by a hand-made stretching step. The pre-stretched sample was then placed in a tight chamber treated with oxygen plasma (Plasma 540/540 Dual Chamber RIE system) at a power of 150 watts, pressure of 500 mTorr for 5mins to generate a thin layer of SiOx on its top surface. One-dimensional wrinkling pattern generated spontaneously at stretching direction after the stretching released. Three identical samples aligned together for next-step mold. The thoroughly degassed but uncured PDMS mixture was then poured over three aligned wrinkling surface and cured at 80° for 1 hour. After cooling to room

temperature, with peeling off from the templated carefully, the PDMS replica with one-dimensional wrinkling surficial pattern are obtained. The replica was then cut prestretched to 20% perpendicular to first wrinkling direction and then place in the UVO cleaner (Jelight model 42) at the distance ~10mm for 1hour to generate a stiff SiOx layer on top surface. After releasing the 20% strain, the one-dimensional-one-dimensional two-layer hierarchical surface morphologies were obtained for potential optical applications such as optical gratings and optical diffusers.

4.1.2 Structural Characterization

Optical microscopy image of one-dimensional/one-dimensional hierarchical structures were obtained by the optical microscope (BX60, Olympus) integrated with CCD camera in a reflection mode. Scanning electron microscopy (SEM) were obtained by a Hitachi SU3500 microscope with an accelerating voltage of 30kV. Surface profiles for micro-leveled wrinkle were measured by Alpha-step 500 surface profilometer (Tencor). Surface profile for nano-leveled wrinkle patterns were measured by atomic force microscope (AFM) with tapping mode.

4.1.3 Optical Characterization

Total and diffusive transmittance of two samples stacking together was measured by the UV-VIS-NIR spectrophotometer (Shimadzu 3101PC) integrated with integrating sphere (Shimadzu ISR 3100). The haze index was

generated by the ratio of diffusive transmittance versus total transmittance. For the optical diffusive patterns, the light source was a collimated green beam with wavelength of 532nm transmitting through the optical diffuser sample. The white screen behind the sample was placed to collect diffusive pattern. The distance from screen to sample was fixed to 43.5mm.

4.2 Fabrication Process

Figure 4-1 schematically exhibits the fabrication process of two-layer wrinkling hierarchical structure. The oxygen plasma first used to etch the pre-stretched polymerized PDMS surface to carry out a thin layer of SiOx. After releasing the strain, the sub-micro-scaled one-dimensional wrinkling patterns can be extracted as a result of the mechanical properties' mismatch between the top SiOx thin layer and PDMS substrate. Then the uncured PDMS was poured over the PDMS template with wrinkling patterns. After carefully peeling off from the molding, the perfect replicated wrinkling surface was obtained since the significant replication characters like low surface energy for cured PDMS polymer. The replica fixed and clamped with a 20% pre-strain along the direction perpendicular to the first replicated wrinkle direction and exposed with the UVO etching for 60mins. After pre-strain was released, the micro-scaled wrinkling patterns propagated perpendicular to first replicated wrinkling direction spontaneously. Therefore, two-layer one-dimensional perpendicular mutually hierarchical

surface morphology can be obtained. Furthermore, by changing the second stretching direction, various surficial morphologies can be generated. Such deformable pattern will be discussed later.

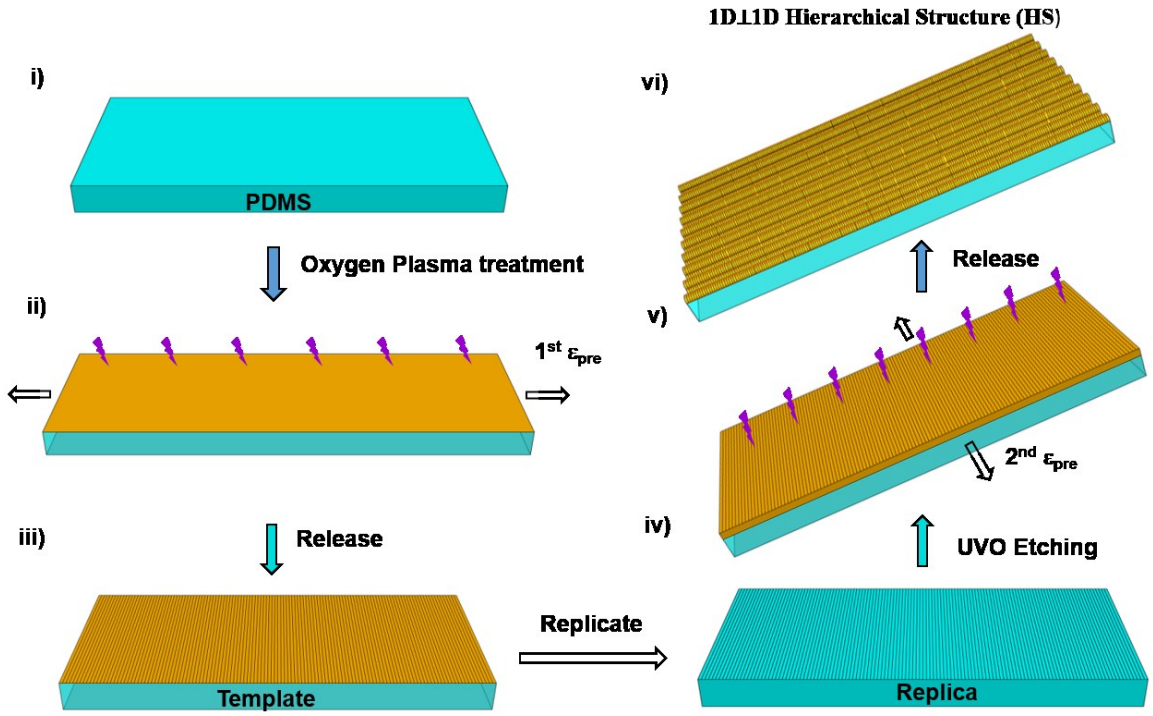

Figure 4-1. Schematic illustration of fabrication process for two-layer hierarchical surface for optical grating application. i) Preparation of freestanding PDMS substrate. ii) Oxygen plasma treatment to pre-strained PDMS to generate a thin layer of SiO_x at the top. iii) After strain released, the one-dimensional wavy PDMS template can be obtained. iv) uncured PDMS was poured over the templated to replicate surface morphology. v) UVO etching to replica to generate another layer of SiO_x at the top after the second pre-strain which is perpendicular to the propagating direction of first wrinkles. vi) After releasing 2nd pre-strain, 1D⊥1D Hierarchical Structure (HS) surface morphology for optical grating can be obtained.

4.3 Surface Morphology and profiles

Figure 4-2a) shows microscopy image of surface transformation from two-layer hierarchical structure to one-layer structure with only one-dimensional

sub-micro-scaled surface morphology. The original surface morphology is a combination of sub-micro-scaled wrinkling patterns perpendicular to micro-scaled wrinkling patterns. With the applied strain along the micro-scaled wrinkling patterns direction increasing from 0% to 20% which is the same with the second stretched strain, the micro-scaled patterns are stretched to flatten continuously while only the replicated sub-micro-scaled wrinkling patterns remain. After the release, the large wrinkles recover to its initial stage. Figure 4-2b) show the SEM image of such hierarchical surface structure which demonstrates that the small wrinkling structure propagated onto the large buckled wavy surface and was also orthogonal to the large wrinkle patterns. Figure 4-2c) shows the surface profile of initial replicated sub-micro-scaled wrinkling structure with an average wavelength of 2.6μm and amplitude of 150nm. Figure 4-2d) shows the surface profile of initial micro-scaled wrinkling pattern with no strain applied. The one-dimensional wavy patterns generate along the y direction uniformly with average wavelength of 90μm and amplitude of 8μm which both much larger than replicated small wrinkles. Figure 4-2e) exhibits the development of wavelength and amplitude of large wrinkles via normal strain applied. As the applied strain increased, the wavelength increased and amplitude decreased which means the surface developed to flatten state at micro-scaled level.

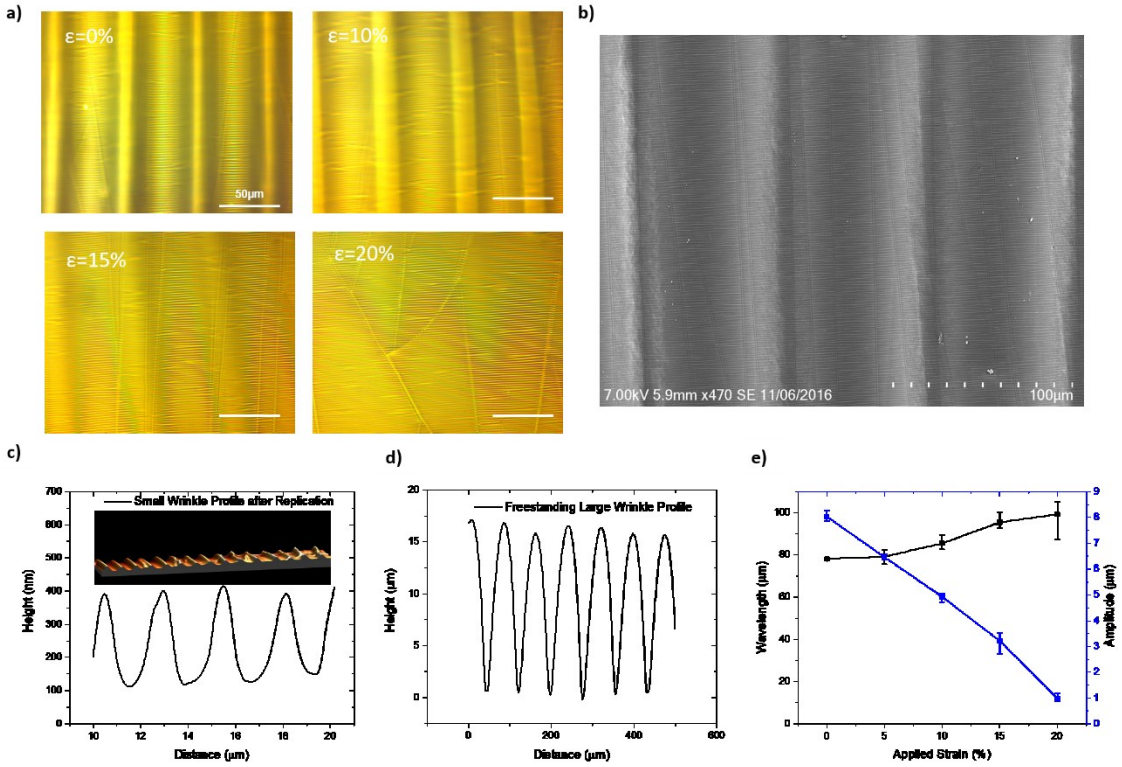

Figure 4-2. Surface morphology and profiles for tunable optical grating. a) Microscopy images of two-layer hierarchical surface morphologies with increasing strain applying. B) Scanning electron microscope (SEM) image for two-layer hierarchical wavy surface morphology with no strain applied from a titled view. c) Wavy profile for replicated sub-micro-scaled wrinkles by atomic force microscope (AFM). d) Surface profile for micro-scaled wrinkles. e) The relationship between wavelength& amplitude of large wrinkles versus increased applied strain.

4.4 Potential Deformable Optical Grating Applications

Nowadays, diffractive optical components have raised a lot of attentions considering their vast potential applications in strain sensors, photonic systems. From novel tunable optical patterns via simple actuation, we demonstrated that the initial diffractive& diffusive patterns from various hierarchical surficial structures can be changed to one-dimensional diffraction patterns without any deficiency for diffraction effect.

To observe the optical patterns, the optical observation system is built up: the monochromatic green laser (532nm) transmit a collimated light going through our optical grating samples, and a white screen behind the sample to detect and collect the optical patterns. Figure 4-3a) shows the optical photography of our sample with orthogonal wrinkling surface when the green light transmitted through the surface, the wavelength of replicated sinusoidal small wrinkles is comparable to the wavelength of transmitting green light (532nm). Here each sinusoidal surficial structure is treated as single slit, all the sinusoidal waves integrated together can form a novel diffraction grating. And larger wrinkling pattern which is much larger than the wavelength of collimated light source contributes a scattering effect for each level diffractive light spot, which means diffractive point light spots have been elongated to light lines paralleled with each other. Therefore, a pattern of the paralleled diffractive light lines generated when a collimated light source whose wavelength is comparable to our small wrinkles' wavelength. Besides, when the sample is stretched from 0% strain to 20% strain which is same as second stretching strain, the paralleled light lines shrink to only diffractive light spots shown in Figure4-3 a). However, the distance between each diffractive maxima spot remains the same which is almost independent to the applied strain. To further investigate the observation, the light intensity distribution of our light patterns is quantitatively analyzed by using ImageJ Software. The Figure 4-3c) exhibit

the light intensity distribution along the vertical direction under various applied normal strains, the distance between the zeroth and first-order diffraction spot almost remain consistent with initial circumstance even though the applied strained reached to 20% as the large wrinkle has been stretched to flattened. The mechanical explanation of such phenomena is that the flattening of large wrinkles and cracklings propagated along the vertical direction both released nearly all strain applied, as a result, the deformation of small sub-micro-scaled wrinkles has been decoupled from the normal stretching. Figure 4-3a) also shows the digital photography of such sample under normal strain applied. The light shrined to diffractive light spots as the stretching engaged in. The deformation along the horizontal direction is much larger than dislocation along vertical direction due to Poisson's Effect, but the diffractive spots are as clear as three spots totally separate with each other at same distance which demonstrates the replicated small wrinkle can survive without flattening even if the normal strain reach to 20%.

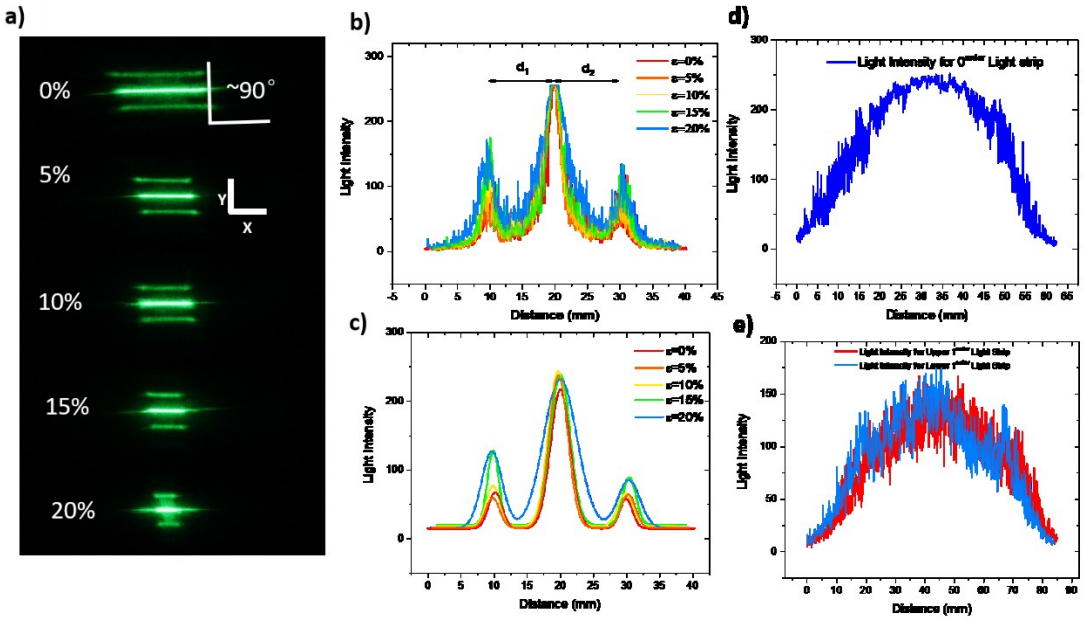

Figure 4-3. Optical performance for deformable optical grating. a) Tunable diffraction& diffusion region with increased applied strain. Initial state for tunable pattern is a paralleled line shape. b) Light Intensity distributions along Y direction for various strain-state optical grating. c) Multiple peak Gaussian curve fitting for various light intensity distributions along Y direction. d) 0 order light intensity distribution along X direction. e) Light intensity distribution along Y direction for upper and lower light stripes.

4.5 Stacking Effect for potential optical diffuser application

Recently, optical diffuser attracted a lot of attention from a variety of industrial applications such as illumination field where there always needs an optical component to soften the light source or minimize and eliminate high intensity bright light spots in small region. In this section, two samples (1D-1D &1D-1D) stack to an integration which can scattering the light evenly in a large region. Furthermore, more general stacking circumstances are discussed later for potential applications.

Figure 4-4 a) shows the diffusive image when 1D-1D&1D-1D orthogonal stacked together. The distance from stacked samples to detected screen is also fixed to 43.5mm. The diffusing pattern is a rectangular-shaped even light region with the scattering angle about horizontally and vertically respectively. The total transmittance and diffusive transmittance are both measure by using a UV-vis-NIR spectrophotometer integrated with an integrating sphere. And haze transmittance is the ratio between the total transmittance and diffusive transmittance. Higher haze transmittance, more significant the scattering effect is. The optical image is also a combination of two single diffusing images since two rough hierarchical stack together without any space. For single 1D⊥1D circumstance, it has paralleled line-shaped pattern, the orthogonal stacking of 1D⊥1D paralleled to 1D⊥1D circumstance will spread out the pattern along vertical direction homogeneously. Both two transmittances have a uniform value within the visible light range (wavelength spectrum from 280nm to 780nm) shown in figure 5-5. The haze index is so high that more than 90% which implicate a high-efficient scattering effect. The uniformity of light intensity distribution along vertical and horizontal direction also exhibited in figure 4-4b) and c) respectively. All in all, the stacking surface morphologies for two identical samples can be used for potential optical diffuser uniformly and productively. Furthermore, various combinations of two samples stacking together has been investigated, for example, the optical image of 1D⊥1D paralleled with

1D∥1D is still three paralleled line-shaped pattern whose central line is brightest, light intensity dropped vertically. But the central line-shaped line spot is much longer and brighter than first order diffraction light spot. Besides, when 1D⊥1D sample and 1D∠45°1D sample integrated together vertically, the combined photography is three parallelogram-shaped bright regions with some overlaps, and when they are horizontal stacking, the enhanced paralleled light strips can be generated.

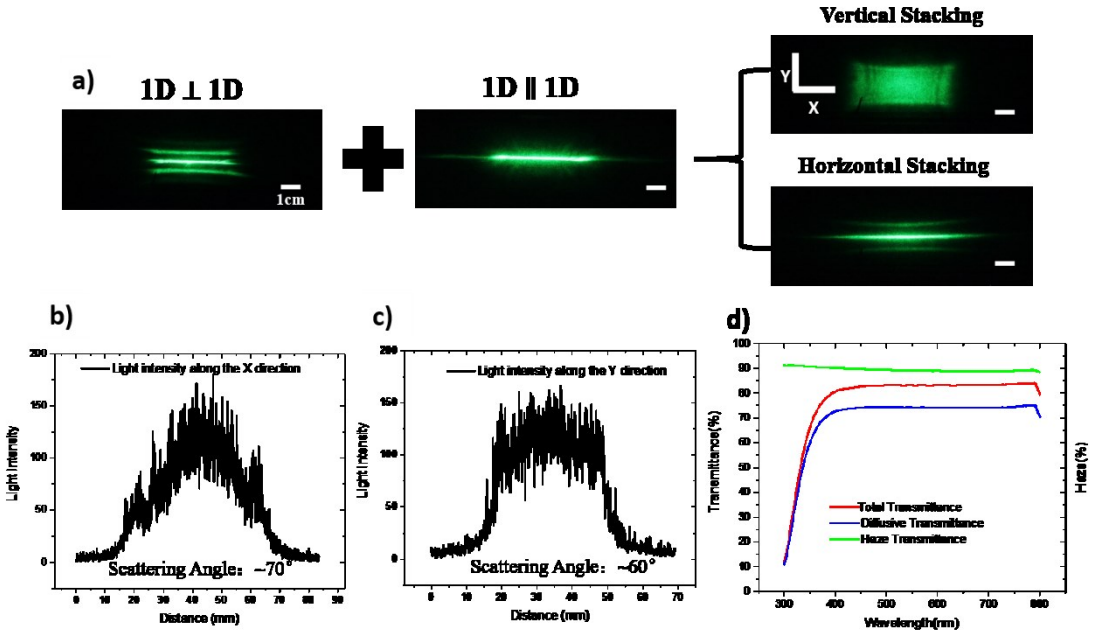

Figure 4-4 Optical performance for stacked optical diffusers. a) Schematic illustration of stacking diffusion effect that 1D⊥1D & 1D∥1D two HS samples stacked vertically and horizontally. b) Light intensity distribution along X direction for vertical stacked samples. c) Light intensity distribution along Y direction for vertical stacked samples. d) Total transmittance, diffusive transmittance, and haze index for vertical stacked optical diffuser.

4.6 Conclusions

In this chapter, a robust, simple, and low-cost approach has been developed to fabricate a two-layered hierarchical surface structure with combination of micro-scaled wrinkles along with sub-micro-scaled sinusoidal wrinkles. Such unique structure has potential contribute to optical grating applications. The initial pattern of optical grating while collimated light going through is three line-shaped light spots paralleling with each other whose central line strip has brightest light intensity, two first order light strips separated by central strip has lower light intensity but same length compared with central diffusion spot. In addition, three diffusion spots shrined spontaneously as an increasing normal stretching applied. Moreover, large diffusion region for two identical samples stacking together with no distance demonstrate its potential for high-performance optical diffuser. The optical exploration of this series of surface morphologies has a profound impact for future optical system design.

Chapter 5 Summary and Prospects

5.1 Summary

In this dissertation, the relationship between the micro-scaled, nano-scaled wrinkling patterns and optical properties has been explored. The PDMS substrate work perfectly as both template and replica. Several optical systems has been developed simply and cheaply for a wide range of applications as optical smart window, optical diffuser, and optical grating. The fabrication methods in this dissertation give inspiration on how to realize simple actuation for tunable optical properties. The dissertation also has a profound and far reaching significance on fabrication of hierarchical surface morphologies and its potential optical applications.

Firstly, in chapter 2, an optimal transmittance performance and range of tunable transmittance for a series of optical smart windows have been proposed since the different UVO treating times lead to different surface morphologies for such fabrication strategy. However, the diffusion region is not general for such surface morphology. Therefore, secondly, the one-dimensional wrinkling surface fabrication approach is combined with template replication to generate a two-dimensional micro-scaled wrinkling surface morphology for potential high-performance tunable optical diffusers. In addition, two-rough-surface optical diffuser has been exhibited to enhance optical performance. How about two scaled wrinkling patterns integrated

together? In chapter 4, the sub-micro-scaled and micro-scaled integrated together to form a two-dimensional surface morphology which is suitable for optical grating. Besides, we demonstrate that two optical gratings stacking together is a high-performance optical diffuser as well.

5.2 Prospects

From the beginning of inspiration, PDMS as a foundation material to support the experimental design due to its high optical transparency, low surface energy, deformation for large mechanical actuation, especially working as superior replication for complicated surface morphology. In the future, more novel active soft materials integrate with PDMS template can possibly realize broader potential applications. For example, the liquid crystal elastomer (LCE) is hybrid material combining ordered liquid crystal and elastic polymer which is very sensitive to light and thermal stimuli for dramatic reversible change of dimension of more than 400%. Integrating PDMS with LCE cannot achieve dramatically tunable optical systems but also some novel soft robots as well. Hydrogel is a soft H_2o-dispersion-medium gelatin which has crosslinked interior structure. Hydrogel is hydrophilic material which is also hydro-holding based on its unique material properties. Combining PDMS with hydrogel can not only serve for optical devices but also has an implication for biomechanics devices since both have good biocompatibility.

Bibliography

[1] X Li, T Gu, B Wei; Gu; Wei (2012). "Dynamic and Galvanic Stability of Stretchable Supercapacitors". *Nano Letters*. 12 (12): 6366–6371.

[2] Wagner, S., & Bauer, S. (2012). Materials for stretchable electronics. *MRS Bulletin*, 37(3), 207-213.

[3] Rogers, J. A., Someya, T., & Huang, Y. (2010). Materials and Mechanics for Stretchable Electronics. *Scienc*e, 327(5973), 1603 LP-1607.

[4] Zhou Jun, Gu Yudong, Fei Peng, Mai Wenjie, Gao Yifan,Yang Rusen, Bao Gang, Wang Zhong Lin (2008). Flexible Piezotronic Strain Sensor. *Nano Letters*, 8(9), 3035–3040.

[5] Amjadi, M., Pichitpajongkit, A., Lee, S., Ryu, S., & Park, I. (2014). Highly Stretchable and Sensitive Strain Sensor Based on Silver Nanowire–Elastomer Nanocomposite. *ACS Nano*, 8(5), 5154–5163.

[6] Manna, U., Carter, M. C. D. and Lynn, D. M. (2013), "Shrink-to-Fit" Superhydrophobicity: Thermally-Induced Microscale Wrinkling of Thin Hydrophobic Multilayers Fabricated on Flexible Shrink-Wrap Substrates. *Adv. Mater*., 25: 3085–3089.

[7] Li, Y., Li, X., Guo, W., Wu, M., & Sun, J. (2016). Spontaneous wrinkling of layer-by-layer assembled polyelectrolyte films for humidity-responsive superhydrophobicity. *Science China Chemistry*, 59(12), 1568–1573.

[8] Bowden, N., Brittain, S., Evans, A.G., Hutchinson, J.W. and Whitesides, G.M., 1998. Spontaneous formation of ordered structures in thin films of metals supported on an elastomeric polymer. *Nature*, 393(6681), pp.146-149.

[9] Chan, E.P., Kundu, S., Lin, Q. and Stafford, C.M., 2010. Quantifying the stress relaxation modulus of polymer thin films via thermal wrinkling. *ACS applied materials & interfaces*, 3(2), pp.331-338.

[10] Birman, V., 2005. Thermally induced bending and wrinkling in large aspect ratio sandwich panels. *Composites Part A: Applied Science and Manufacturing*, 36(10), pp.1412-1420.

[11] Khang, D.Y., Jiang, H., Huang, Y. and Rogers, J.A., 2006. A stretchable form of single-crystal silicon for high-performance electronics on rubber substrates. *Science*, 311(5758), pp.208-212.

[12]Choi, W.M., Song, J., Khang, D.Y., Jiang, H., Huang, Y.Y. and Rogers, J.A., 2007. Biaxially stretchable "wavy" silicon nanomembranes. *Nano Letters*, 7(6), pp.1655-1663.

[13] Xiao, J., Jiang, H., Khang, D.Y., Wu, J., Huang, Y. and Rogers, J.A., 2008. Mechanics of buckled carbon nanotubes on elastomeric substrates. *Journal of Applied Physics*, 104(3), p.033543.

[14] Xiao, J., Ryu, S.Y., Huang, Y., Hwang, K.C., Paik, U. and Rogers, J.A., 2010. Mechanics of nanowire/nanotube in-surface buckling on elastomeric substrates. *Nanotechnology*, 21(8), p.085708.

[15] Moon, M.W., Lee, S.H., Sun, J.Y., Oh, K.H., Vaziri, A. and Hutchinson, J.W., 2007. Wrinkled hard skins on polymers created by focused ion beam. *Proceedings of the National Academy of Sciences*, 104(4), pp.1130-1133.

[16] Yang, S., Khare, K. and Lin, P.C., 2010. Harnessing surface wrinkle patterns in soft matter. *Advanced Functional Materials*, 20(16), pp.2550-2564.

[17] Chiche, A., Stafford, C.M. and Cabral, J.T., 2008. Complex micropatterning of periodic structures on elastomeric surfaces. *Soft Matter*, 4(12), pp.2360-2364.

[18] Efimenko, K., Rackaitis, M., Manias, E., Vaziri, A., Mahadevan, L. and Genzer, J., 2005. Nested selfsimilar wrinkling patterns in skins. *Nature materials*, 4(4), pp.293-297.

[19] Lin, P.C. and Yang, S., 2007. Spontaneous formation of one-dimensional ripples in transit to highly ordered two-dimensional herringbone structures through sequential and unequal biaxial mechanical stretching. *Applied physics letters*, 90(24), p.241903.

[20] Guo, C.F., Nayyar, V., Zhang, Z., Chen, Y., Miao, J., Huang, R. and Liu, Q., 2012. Path‐Guided Wrinkling of Nanoscale Metal Films. *Advanced Materials*, 24(22), pp.3010-3014.

[21] Bae, H.J., Bae, S., Park, C., Han, S., Kim, J., Kim, L.N., Kim, K., Song, S.H., Park, W. and Kwon, S., 2015. Biomimetic Microfingerprints for Anti‐Counterfeiting Strategies. *Advanced Materials*, 27(12), pp.2083-2089.

[22] Ohzono, T., Matsushita, S.I. and Shimomura, M., 2005. Coupling of wrinkle patterns to microspherearray lithographic patterns. *Soft Matter*, 1(3), pp.227-230.

[23] Kim, H.S. and Crosby, A.J., 2011. Solvent‐Responsive Surface via Wrinkling Instability. *Advanced materials*, 23(36), pp.4188-4192.

[24] Chung, J.Y., Nolte, A.J. and Stafford, C.M., 2009. Diffusion‐Controlled, Self‐Organized Growth of Symmetric Wrinkling Patterns. *Advanced Materials*, 21(13), pp.1358-1362.

[25] Song, J., Jiang, H., Choi, W.M., Khang, D.Y., Huang, Y. and Rogers, J.A., 2008. An analytical study of two-dimensional buckling of thin films on compliant substrates. *Journal of Applied Physics*, 103(1), p.014303.

[26] Baetens, R.; Jelle, B.P.; Gustavsen, A. (2010). "Properties, requirements and possibilities of smart windows for dynamic daylight and solar energy control in buildings: A state-of-the-art review". *Solar Energy Materials and Solar Cells*. 94 (2): 87–105.

[27] Lee, E.S.; Tavil, A. (2007). "Energy and visual comfort performance of electrochromic windows with overhangs". *Building and Environment*. **42** (6): 2439–2449.

[28] Loonen, R.C.G.M.; Singaravel, S.; Trcka, M; Costola, D; Hensen, J.L.M. (2014). "Simulation-based support for product development of innovative building envelope components". *Automation in Construction*. **45**: 86–95.

[29] Casini, Marco (2016-05-27). Smart Buildings: Advanced Materials and Nanotechnology to Improve Energy-Efficiency and Environmental Performance. *Woodhead Publishing*. ISBN 9780081006405.

[30] Llordés, A.; Garcia, G.; Gazquez, J.; Milliron, D. J. (2013). "Tunable near-infrared and visible-light transmittance in nanocrystal-in-glass composites". *Nature*. 500 (7462): 323.

[31] Sheraw, C.D., Zhou, L., Huang, J.R., Gundlach, D.J., Jackson, T.N., Kane, M.G., Hill, I.G., Hammond, M.S., Campi, J., Greening, B.K. and Franci, J., 2002. Organic thin-film transistor-driven 104 polymer-dispersed liquid crystal displays on flexible polymeric substrates. *Applied Physics Letters*, 80(6), p.1088.

[32] Granqvist, C.G., 2014. Electrochromics for smart windows: Oxide-based thin films and devices. *Thin Solid Films*, 564, pp.1-38.

[33] Vergaz, R., Sanchez-Pena, J.M., Barrios, D., Vazquez, C. and Contreras-Lallana, P., 2008. Modelling and electro-optical testing of suspended particle devices. *Solar Energy Materials and Solar Cells*, 92(11), pp.1483-1487.

[34] Dyer, A.L., Grenier, C.R. and Reynolds, J.R., 2007. A Poly (3, 4-alkylenedioxythiophene) Electrochromic Variable Optical Attenuator with Near-Infrared Reflectivity Tuned Independently of the Visible Region. *Advanced Functional Materials*, 17(9), pp.1480-1486.

[35] Bechinger, C., Ferrer, S., Zaban, A., Sprague, J. and Gregg, B.A., 1996. Photoelectrochromic windows and displays. Nature, 383(6601), pp.608-610.

[36] Ge, D., Lee, E., Yang, L., Cho, Y., Li, M., Gianola, D. S. and Yang, S. (2015), A Robust Smart Window: Reversibly Switching from High Transparency to Angle-Independent Structural Color Display. *Adv. Mater.,* 27: 2489–2495.

[37] Lee, S.G., Lee, D.Y., Lim, H.S., Lee, D.H., Lee, S. and Cho, K., 2010. Switchable transparency and wetting of elastomeric smart windows. Advanced materials, 22(44), pp.5013-5017.

[38] Ki-Woo, J., Jong-Nam, K., Jin-Young, J., & Il-Kwon Oh. (2017). Wrinkled graphene-AgNWs hybrid electrodes for smart window. *Micromachines, 8*(2), 43.

[39] Walecki, Wojciech, and Peter Walecki. "Robust diffuser and roughness metrology tool for LED manufacturing." SPIE OPTO. *International Society for Optics and Photonics*, 2015.

[40] Golub, M. A., Averbuch, A., Nathan, M., Zheludev, V. A., Hauser, J., Gurevitch, Kagan, A. (2016). Compressed sensing snapshot spectral imaging by a regular digital camera with an added optical diffuser. *Applied Optics*, *55*(3), 432–443.

[41] Kim, G. (2005). A PMMA composite as an optical diffuser in a liquid crystal display backlighting unit (BLU). *European Polymer Journal*, *41*(8), 1729–1737.

[42] Mahpeykar, S. M., Zhao, Y., Li, X., Yang, Z., Xu, Q., Lu, Z.-H., Sargent, Edward, Wang, X. (2017). Cellulose Nanocrystal: Polymer Hybrid Optical Diffusers for Index-Matching-Free Light Management in Optoelectronic Devices. *Advanced Optical Materials*, *5*(21), 1700430–n/a.

[43] Alqurashi, T., Sabouri, A., Yetisen, A. K., & Butt, H. (2017). Nanosecond pulsed laser texturing of optical diffusers. *AIP Advances*, 7(2), 25313.

[44] Butt, H., Knowles, K. M., Montelongo, Y., Amaratunga, G. A. J., & Wilkinson, T. D. (2014). Devitrite-Based Optical Diffusers. *ACS Nano*, 8(3), 2929–2935.

[45] Colombo, Annalisa, et al. "Nanoparticle-doped large area PMMA plates with controlled optical diffusion." *Journal of Materials Chemistry* C 1.16 (2013): 2927-2934.

[46] Liu, Xiao, et al. "Fast fabrication of a novel transparent PMMA light scattering materials with high haze by doping with ordinary polymer." *Optics express* 23.14 (2015): 17793-17804.

[47] Hu, Jingang, Yuming Zhou, and Xiaoli Sheng. "Optical diffusers with enhanced properties based on novel polysiloxane@ CeO 2@ PMMA fillers." *Journal of Materials Chemistry* C 3.10 (2015): 2223- 2230.

[48] Huang, Tzu-Chien, et al. "Fast fabrication of integrated surface-relief and particle-diffusing plastic diffuser by use of a hybrid extrusion roller embossing process." *Optics express* 16.1 (2008): 440-447.

[49] Hu, Jingang, et al. "Optical diffusers based on the novel fillers of polysiloxane@ boehmite core–shell microspheres." *Materials Letters* 165 (2016): 107-110.

[50] Chang, Sung-Il, et al. "Microlens array diffuser for a light-emitting diode backlight system." *Optics letters* 31.20 (2006): 3016-3018.

[51] Bitterli, Roland, et al. "Fabrication and characterization of linear diffusers based on concave micro lens arrays." *Optics express* 18.13 (2010): 14251-14261.

[52] Park, Hyoung-Ghi, and Dahl-Young Khang. "High-performance light diffuser films by hierarchical buckling-based surface texturing combined with internal pores generated from physical gelation induced phase separation of binary polymer solution." *Polymer* 99 (2016): 1-6.

[53] Ohzono, Takuya, et al. "Tunable optical diffuser based on deformable wrinkles." *Advanced Optical Materials* 1.5 (2013): 374-380.

[54] Kang, Gumin, et al. "Broadband and ultrahigh optical haze thin films with self-aggregated alumina nanowire bundles for photovoltaic applications." *Energy & Environmental Science* 8.9 (2015): 2650- 2656.

[55] Baek, Seunghwa, et al. "Improvement of light extraction efficiency in flip-chip light emitting diodes on SiC substrate via transparent haze films with morphology-controlled collapsed alumina nanorods." *ACS applied materials & interfaces* 8.1 (2015): 135-141.

[56] Jui-Hao Wang, Shui-Yang Lien, Jeng-Rong Ho, Teng-Kai Shih, Chia-Fu Chen, Chien-Chung Chen, Wha-Tzong Whang, “Optical diffusers based on silicone emulsions,” *In Optical Materials*, Volume 32, Issue 2, 2009, pp. 374-377.

[57] Kinoshita, S.; Yoshioka, S.; Miyazaki, J. (2008). "Physics of structural colors". Reports on *Progress in Physics*. 71 (7): 076401.

[58] AK Yetisen; H Butt; F da Cruz Vasconcellos; Y Montelongo; CAB Davidson; J Blyth; JB Carmody; S Vignolini; U Steiner; JJ Baumberg; TD Wilkinson; CR Lowe (2013). "Light-

Directed Writing of Chemically Tunable Narrow-Band Holographic Sensors". *Advanced Optical Materials*. **2** (3): 250–254.

[59] Lockyear, M. J., Hibbins, A. P., White, K. R., & Sambles, J. R. (2006). One-way diffraction grating. *Physical Review E*, 74(5), 56611.

[60] Moiseyenko, R. P., Herbison, S., Declercq, N. F., & Laude, V. (2012). Phononic crystal diffraction gratings. *Journal of Applied Physics*, 111(3), 34907.

[61] Vörös, J., Ramsden, J. J., Csúcs, G., Szendrő, I., De Paul, S. M., Textor, M., & Spencer, N. D. (2002). Optical grating coupler biosensors. *Biomaterials*, 23(17), 3699–3710.

[62] Prikockis, M., Wijesinghe, H., Chen, A., VanCourt, J., Roderick, D., & Sooryakumar, R. (2016). An on-chip colloidal magneto-optical grating. *Applied Physics Letters*, 108(16), 161106.

[63] Chen, X., Wu, Y., Yu, A., Xu, L., Zheng, L., Liu, et al. (2017). Self-powered modulation of elastomeric optical grating by using triboelectric nanogenerator. *Nano Energy*, 38(Supplement C), 91–100.

[64] Teng Ma, Hanshuang Liang, George Chen, Benny Poon, Hanqing Jiang, and Hongbin Yu, "Micro-strain sensing using wrinkled stiff thin films on soft substrates as tunable optical grating," *Opt. Express 21*, 11994-12001 (2013)

[65] Gutruf, P., Zeller, E., Walia, S., Sriram, S. and Bhaskaran, M., 2015. Mechanically Tunable High Refractive-Index Contrast TiO2–PDMS Gratings. *Advanced Optical Materials*, 3(11), pp.1565-1569.

[66] Z. Li, Y. Zhai, Y. Wang, G. M. Wendland, X. Yin, J. Xiao, Harnessing Surface Wrinkling–Cracking Patterns for Tunable Optical Transmittance, *Advanced Optical Materials*, 2017, 5, 1700425.

[67] Z. Li, Doctoral Dissertation: Stretchable and Tunable Optical Systems Based on Surface Morphologies, *ProQuest Dissertations & Theses*, 2017